

THE EFFECT OF $1/Q^2$ AND α_s CORRECTIONS ON TESTS OF QCD*

L. F. Abbott[†] and R. Michael Barnett
Stanford Linear Accelerator Center
Stanford University, Stanford, California 94305

ABSTRACT

We discuss in detail the use of the structure function $F_3(x, Q^2)$ of deep-inelastic neutrino scattering for testing quantum chromodynamics. We show that higher-twist (order $1/Q^2$) contributions which are commonly neglected can have a dramatic impact on tests of QCD. With or without such contributions, QCD is entirely consistent with all data. At present the data are not accurate enough to determine the magnitudes of these $1/Q^2$ contributions within the context of QCD. Furthermore, the possible presence of higher-twist terms makes it impossible to unambiguously detect the logarithmic Q^2 dependence and anomalous dimensions which distinguish QCD from hypothetical alternative theories. As a result, more precise data with higher Q^2 are needed to provide definitive tests of QCD. The corrections of second-order in α_s introduce fewer complications for testing QCD, and provide a useful context for understanding critical ambiguities in the definitions of α_s and Λ .

Submitted to Annals of Physics

* Work supported by the Department of Energy under contract number EY-76-C-03-0515.

† Address after September 1979: Physics Department, Brandeis University, Waltham, Mass. 02154.

I. INTRODUCTION

Scaling violations in deep-inelastic structure functions provide an important means of investigating the validity of quantum chromodynamics (QCD) as a theory of the strong interactions [1]. In deep-inelastic scattering processes such as $\nu N \rightarrow \mu + \text{anything}$, $eN \rightarrow e + \text{anything}$ and $\mu N \rightarrow \mu + \text{anything}$ (see Fig. 1), the cross-section can be written in terms of products of leptonic and hadronic pieces:

$$\frac{d^2\sigma}{dE' d\Omega'} \propto \ell_{\mu\nu} W^{\mu\nu} \quad (1.1)$$

The hadronic part is the Fourier transform of the spin-averaged nucleon matrix element of weak or electromagnetic currents

$$W_{\mu\nu} = \frac{1}{2\pi} \int d^4x e^{iq \cdot x} \langle \vec{p} | J_{\mu}^{\dagger}(x) J_{\nu}(0) | \vec{p} \rangle \quad (1.2)$$

spin
averaged

If the current J_{μ} is conserved or if we neglect lepton mass terms in the cross-sections, then the most general form for $W_{\mu\nu}$ is

$$W_{\mu\nu} = \left(-g_{\mu\nu} + \frac{q_{\mu}q_{\nu}}{q^2} \right) F_1 + \frac{1}{(p \cdot q)} \left(p_{\mu} - q_{\mu} \frac{p \cdot q}{q^2} \right) \left(p_{\nu} - q_{\nu} \frac{p \cdot q}{q^2} \right) F_2$$

$$- \frac{i}{2(p \cdot q)} \epsilon_{\mu\nu\alpha\beta} p^{\alpha} q^{\beta} F_3 \quad (1.3)$$

The three structure functions $F_i(q^2, p \cdot q)$ reflect the dynamics of the nucleon-current interaction.

The parton model predicts that the structure functions should "scale" [2] in Q^2 for large Q^2 :

$$F_i(x, Q^2) = F_i(x) \quad (1.4)$$

where $Q^2 \equiv -q^2$ and $x = Q^2/2p \cdot q$. In QCD, however, a mild violation of this scaling is expected [1] and is evidenced by the presence of terms proportional to inverse powers of $\ln Q^2$. The scaling violation can be thought of as resulting from gluon radiation and quark-antiquark pair production during the scattering process [3].

In this paper, our attention will be focused on the structure function F_3 , but most of our results and conclusions are applicable to the study of the other structure functions as well. Since F_3 reflects only the flavor-nonsinglet part of the interaction, the QCD analysis of F_3 is less complex and hence easier to discuss than that for F_1 or F_2 . More importantly, the QCD predictions for F_3 do not depend on the gluon distribution inside the nucleon which cannot be directly measured; i.e., diagrams such as Fig. 2 make no contribution to F_3 . F_3 can be extracted from deep-inelastic neutrino scattering experiments, since for isoscalar targets

$$xF_3 \propto \frac{d^2\sigma^{\nu}}{dE' d\Omega'} - \frac{d^2\sigma^{\bar{\nu}}}{dE' d\Omega'} \quad (1.5)$$

F_3 arises from VA interference terms. Since there are no such terms in eN or μ N scattering processes (which are parity-conserving), the analysis of F_3 is restricted to ν N scattering.

We use two separate approaches in examining QCD. The first approach uses the QCD predictions [3] for the Q^2 -evolution of $xF_3(x, Q^2)$. If there were no scaling violations, then $Q^2 \frac{\partial}{\partial Q^2} xF_3(x, Q^2) = 0$. The gluon radiation and quark pair production which arise in QCD are proportional to $\alpha_s(Q^2)$ and lead to the following differential equation which describes the behavior of xF_3 to lowest-order in the running coupling constant $\alpha_s(Q^2)$:

$$Q^2 \frac{\partial}{\partial Q^2} xF_3(x, Q^2) = \frac{\alpha_s^o(Q^2)}{2\pi} \int_x^1 dw \left(\frac{x}{w}\right) wF_3(w, Q^2) P_{q \rightarrow q}\left(\frac{x}{w}\right) \quad (1.6a)$$

$\frac{\alpha_s^o(Q^2)}{2\pi} P_{q \rightarrow q}\left(\frac{x}{w}\right)$ is the probability of seeing a quark of momentum fraction x arising from a quark of momentum fraction w as in Fig. 3, when probing with momentum Q^2 . $P_{q \rightarrow q}$ can be calculated in QCD and when this result is substituted into Eq. (1.6a) we find

$$Q^2 \frac{\partial}{\partial Q^2} xF_3(x, Q^2) = \frac{\alpha_s^o(Q^2)}{3\pi} \left\{ [3 + 4\ell_n(1-x)] xF_3(x, Q^2) + \int_x^1 dw \frac{2}{(1-w)} \left[(1+w^2) \frac{x}{w} F_3\left(\frac{x}{w}, Q^2\right) - 2xF_3(x, Q^2) \right] \right\} \quad (1.6b)$$

The coupling constant $\alpha_s(Q^2)$ in QCD is given to lowest order by

$$\alpha_s^o(Q^2) = \frac{4\pi}{\beta_0 \ell_n Q^2 / \Lambda^2} \quad (1.7)$$

with

$$\beta_0 = 11 - \frac{2}{3} N_f \quad (1.8)$$

where N_f is the number of quark flavors and Λ is a free parameter. It is the asymptotically free behavior of $\alpha_s(Q^2)$ in Eq. (1.7) which gives the logarithmic dependence on Q^2 typical of QCD.

Although QCD predicts the Q^2 -evolution of xF_3 , it does not completely specify a boundary condition for Eq. (1.6). One could use the data for xF_3 at a particular Q^2 value, $Q^2 = Q_0^2$, as a boundary condition and integrate Eq. (1.6) to obtain predictions for other Q^2 values.

However, in this approach the entire QCD prediction for all Q^2 is based on a small fraction of the data taken at $Q^2 = Q_0^2$ and a true global fit of the data is impossible. We choose instead to assume a form like

$$xF_3(x, Q_0^2) = C x^a (1-x)^b \quad (1.9)$$

at some reference point $Q^2 = Q_0^2$, integrate Eq. (1.6) to determine xF_3 at other Q^2 values and fit the data at all Q^2 to determine the best values for the parameters in Eq. (1.9). This allows us to use all the data to decide on the best boundary condition for Eq. (1.6).

The Q^2 -evolution approach provides a clear visual interpretation of scaling violation. One can observe the impact of exclusive channels although it is difficult to account for them quantitatively. A disadvantage of this approach is that it depends on assuming a form like Eq. (1.9) for $xF_3(x, Q^2)$ in order to obtain a global fit.

The second approach we will use to study QCD involves taking moments of xF_3 defined by [4]

$$M_3(N, Q^2) = \int_0^1 dx x^{N-2} xF_3(x, Q^2) \quad (1.10)$$

The QCD calculation of the moments of xF_3 using the Wilson operator product expansion [5] is discussed in detail in Section II. Alternatively the moments can be obtained by applying $\int_0^1 dx x^{N-2}$ to both sides of the evolution equation (Eq. (1.6)). Performing the integrals, one finds

$$Q^2 \frac{\partial}{\partial Q^2} M_3(N, Q^2) = -\frac{\alpha_s^0}{8\pi} \gamma_0^N M_3(N, Q^2) \quad (1.11)$$

where γ_0^N are the anomalous dimensions defined by

$$\gamma_0^N = -4 \int_0^1 dw w^{N-1} P_{q \rightarrow q}(w) \quad (1.12)$$

and in QCD

$$\gamma_0^N = \frac{8}{3} \left(1 - \frac{2}{N(N+1)} + 4 \sum_{j=2}^N \frac{1}{j} \right) \quad (1.13)$$

The solution to Eq. (1.11) is

$$M_3(N, Q^2) = M_3(N, Q_0^2) \left(\frac{\alpha_s^o(Q^2)}{\alpha_s^o(Q_0^2)} \right)^{d_N} \quad (1.14)$$

with

$$d_N \equiv \frac{\gamma_0^N}{2\beta_0} \quad (1.15)$$

Using Eq. (1.7) one obtains

$$M_3(N, Q^2) = \frac{K_N}{(\ln Q^2/\Lambda^2)^{d_N}} \quad (1.16)$$

The K_N are unknown constants which must be determined from the data. This approach provides very clean predictions which do not depend on any assumptions about the x -dependence of xF_3 such as Eq. (1.9). This allows for quantitative checks of the logarithmic behavior and the anomalous dimensions predicted by QCD. The moments smooth out the effects of exclusive channels. Whether this allows one to account for the impact of these channels is not clear. If data are not available over the entire x range and in particular all the way out to $x=1$, the moments cannot be determined without extrapolating the data. Finally, all moments for $N \geq 4$ heavily weight contributions at high x ($x > 0.5$) and neglect low x contributions.

As one can see from Eqs. (1.6), (1.7), and (1.16), crucial features of QCD are the logarithmic dependence on Q^2 and the definite predictions of Eqs. (1.8), (1.13), and (1.15) for the powers d_N . In phenomenological studies of QCD, one must verify that these two features are clearly indicated by the data. Thus, in Section IV we will ask whether the data require a form such as Eq. (1.16) as opposed to moments which are independent of Q^2 or which vary with inverse powers of Q^2 . These alternatives do not at present represent viable strong interaction theories, but are merely used to determine whether there is evidence for the logarithmic behavior characteristic of QCD. Similarly, in Section IV we will investigate whether the d_N are sufficiently determined by the data to imply a test of QCD.

It would be quite straightforward to distinguish the logarithmic behavior of QCD in deep-inelastic data if it were not for the fact that the QCD predictions are subject to several types of corrections. These include target-mass corrections [6-8], higher-twist effects and corrections [9,10] of higher order in α_s . We begin by discussing the target mass effects.

The QCD predictions discussed above are derived under the assumption that the nucleon mass squared, m_p^2 , is negligible compared to Q^2 . At low Q^2 (where much of present data is taken) this is not the case and there are correction terms of order m_p^2/Q^2 . These are discussed in the context of the operator product expansion in Section II. It is also instructive to discuss target-mass corrections in the language of the parton model [7,8]. If the target nucleon is moving in the x_3 direction, then the relevant quantity for deep-inelastic scattering is

$$\tilde{x} = \frac{(p_0 + p_3)_{\text{quark}}}{(p_0 + p_3)_{\text{nucleon}}} \quad . \quad (1.17)$$

An expression for \tilde{x} can be derived by taking the final struck quark to be on mass-shell and massless. If we ignore proton mass terms, this leads to the result

$$\tilde{x} = x = \frac{Q^2}{2p \cdot q} \quad . \quad (1.18)$$

However, if we keep all proton mass terms we obtain the ξ -scaling variable

$$\tilde{x} = \xi = \frac{2x}{1 + \sqrt{1 + \frac{4m_p^2 x^2}{Q^2}}} \quad . \quad (1.19)$$

Note that as $m_p^2/Q^2 \rightarrow 0$ we find $\xi \rightarrow x$. If target mass effects are taken into account, the predictions for $x F_3$ can be written in terms of a new function $F(x, Q^2)$ as was first discussed by Georgi and Politzer [7].

Defining

$$v = \left(1 + \frac{4m_p^2 x^2}{Q^2} \right)^{-1/2} \quad (1.20)$$

we have

$$xF_3(x, Q^2) = \frac{x^2 v^2}{\xi^2} F(\xi, Q^2) + \frac{4m_p^2 x^3 v^3}{Q^2} \int_{\xi}^1 dx' \frac{F(x', Q^2)}{x'^2} \quad . \quad (1.21)$$

Again, for $Q^2 \gg m_p^2$,

$$xF_3(x, Q^2) \xrightarrow[Q^2 \gg m_p^2]{} F(x, Q^2) \quad . \quad (1.22)$$

Whereas in the x-scaling case it was xF_3 which obeyed the evolution Eq. (1.6), it is now the function F which obeys the evolution equation of QCD,

$$Q^2 \frac{\partial}{\partial Q^2} F(x, Q^2) = \frac{\alpha_s^0(Q^2)}{3\pi} \left\{ [3 + 4\ln(1-x)] F(x, Q^2) + \int_x^1 dw \frac{2}{(1-w)} \left[(1+w^2) F\left(\frac{x}{w}, Q^2\right) - 2F(x, Q^2) \right] \right\}. \quad (1.23)$$

As before, in order to integrate the evolution equation we will assume a form for F at a starting point $Q^2 = Q_0^2$. Again, we will make the assumption

$$F(x, Q_0^2) = C x^a (1-x)^b. \quad (1.24)$$

Target mass corrections also affect the QCD predictions for moments. The result, discussed in Section II is that the QCD form remains unchanged:

$$\tilde{M}_3(N, Q^2) = \frac{K_N}{(\ln Q^2/\Lambda^2)^{d_N}} \quad (1.25)$$

but the definition of the moment used on the left-hand side of Eq. (1.25) changes from the simple definition of Eq. (1.10) to the Nachtmann form [6]

$$\tilde{M}_3(N, Q^2) = \int_0^1 dx \frac{\xi^{N+1}}{x^3} xF_3(x, Q^2) \frac{1 + (N+1) \sqrt{1 + \frac{4m_p^2 x^2}{Q^2}}}{(N+2)} \quad (1.26)$$

where ξ is defined as in Eq. (1.19). It is straightforward to verify that the ordinary moments of Eq. (1.10) and the Nachtmann moments of Eq. (1.26) become equal as $m_p^2/Q^2 \rightarrow 0$. However, at low Q^2 ($Q^2 \lesssim 3 \text{ GeV}^2$)

the differences between them become quite large as we show in Section III.

Although the ξ -scaling scheme correctly accounts for target-mass effects, it does not correctly describe the final-state kinematics of deep-inelastic scattering [11]. For example, in the parton-model discussion above we have taken into account the initial nucleon mass, but we have ignored the fact that the final-state hadronic mass must be greater than m_p . This results in problems for the ξ -scaling description of xF_3 in the region near $x=1$. Kinematics requires that xF_3 vanish for $x > 1$. One might therefore choose a function $F(\xi, Q_0^2)$ which vanishes for $\xi > \xi_{\max}$ where ξ_{\max} is the value of ξ which corresponds to $x=1$ for $Q^2 = Q_0^2$. This would assure that $xF_3(x, Q_0^2)$ would vanish for $x > 1$. However, this approach can have disastrous consequences. For example, if we take $Q_0^2 = 1 \text{ GeV}^2$ then $\xi_{\max} = 0.64$. We would then find by integrating Eq. (1.23) that $F(\xi, Q^2)$ would vanish for $\xi > 0.64$ at all other Q^2 values as well. At large Q^2 where the ξ - and x -scaling schemes become identical this would lead to the nonsensical prediction $xF_3(x, Q^2) = 0$ for $x > .64$. A more sensible approach then is to take a form like Eq. (1.24) for $F(\xi, Q_0^2)$ which does not vanish for $\xi > \xi_{\max}$. However, when this is done xF_3 will not satisfy the kinematic requirement $xF_3 = 0$ for $x > 1$.

Because the ξ -scaling predictions of Eqs. (1.19)-(1.21) do not vanish at $x=1$ we have the paradoxical situation that in the phenomenology of ξ -scaling we are fitting a form to the data which cannot possibly work. Of course, it is also true that the x -scaling scheme with $xF_3 \propto (1-x)^b$ cannot account for elastic scattering which occurs at $x=1$. In Fig. 4, we show an x -scaling curve (solid curve) and the corresponding

ξ -scaling prediction (dashed curve) compared with BEBC-Gargamelle data [12] at $Q^2 = 1.7 \text{ GeV}^2$. The x -scaling curve fits the inelastic data fairly well in the large x region whereas the ξ -scaling curve overshoots that data considerably as $x \rightarrow 1$. The paradox is somewhat resolved by noting that the ξ -scaling variable acts much like the scaling variable of Bloom and Gilman [13]. One can argue [14] on phenomenological grounds that, in overshooting the data near $x=1$, ξ -scaling may account for the elastic scattering contribution (and resonance contributions) in the sense that the excess area under the ξ -scaling curve equals the area under the elastic peak at $x=1$. In Figs. 4 and 5 we have plotted the elastics in an extra bin from $x=1$ to $x=1.1$ so that this can be visualized. The area under the data point in this bin is equal to the area under the elastic spike at $x=1$ in the original data. It is clear that in fitting the ξ -scaling predictions to the data the elastic contribution must somehow be included. In the case of moments, one possible approach is to include elastics in the integral, Eq. (1.26). In direct fits of xF_3 , however, the elastics remain a more serious problem especially when $Q^2 \lesssim 3 \text{ GeV}^2$ (where elastics contribute significantly). Figure 5 shows the x - and ξ -scaling curves and the elastics at $Q^2 = 3.9 \text{ GeV}^2$. Note that at this larger Q^2 value the solid and dashed curves are converging and the elastics are insignificant.

Unfortunately, target-mass corrections are not the only effects of order $1/Q^2$ which can modify the QCD predictions in deep-inelastic scattering. There are other order $1/Q^2$ effects coming from non-leading-twist operators in the operator product expansion as discussed in Section II. These effects are departures from the simple parton-model picture

because they account for the exchange of gluons between struck and spectator quarks, and other coherent phenomena such as multi-quark scattering, elastic scattering, transverse-momentum effects, resonance production, and constituent meson scattering. In Section IV we will show that higher-twist operators can cause major problems in testing QCD.

These higher-twist effects are expected (using quark-counting arguments [15]) to modify the basic form of xF_3 to something like

$$xF_3(x, Q_0^2) = C x^a (1-x)^b \left[1 + \sum_{j=1}^{\infty} \left(\frac{\mu_j^2}{Q_0^2 (1-x)} \right)^j \right] \quad (1.27)$$

although the exact x dependence of the higher-twist terms is not known. Similarly one expects a modified prediction for the Nachtmann moments (Eq. (1.26)):

$$\tilde{M}_3(N, Q^2) = \frac{K_N}{(\ln Q^2/\Lambda^2)^{d_N}} \left[1 + \sum_{j=1}^{\infty} \left(\frac{\mu_j^2}{Q^2} \right)^j A_j \right] . \quad (1.28)$$

The magnitude of the masses μ_j appearing in Eqs. (1.27) and (1.28) are unknown. The A_j depend on $\ln Q^2/\Lambda^2$ representing the asymptotic freedom corrections to the higher-twist operators. The modifications in the predictions for xF_3 and $\tilde{M}_3(N, Q^2)$ (Eqs. (1.27) and (1.28)) make it quite difficult to unambiguously detect the characteristic logarithmic Q^2 dependence of QCD or the predicted values of d_N (or equivalently, of the anomalous dimension γ_0^N). Distinguishing between $\ln Q^2$ and $1/Q^2$ effects is in fact impossible using present data as we will show in Section IV.

Finally there are corrections to the basic QCD predictions coming from terms of higher-order in α_s which have recently been computed by Floratos, Ross and Sachrajda [9] and by Bardeen, Buras, Duke and Muta [10]. As discussed in Section II in the context of the operator-product expansion, the lowest-order QCD predictions for moments (Eqs. (1.14) and (1.16)) are modified by order α_s corrections to:

$$M_3(N, Q^2) = M_3(N, Q_0^2) \left(\frac{\alpha_s(Q^2)}{\alpha_s(Q_0^2)} \right)^{d_N} \left(1 + \frac{\beta_0 A_N}{4\pi} [\alpha_s(Q^2) - \alpha_s(Q_0^2)] \right) \quad (1.29)$$

At second-order, one can write α_s as

$$\alpha_s(Q^2) = \alpha_s^0(Q^2) \left(1 - \frac{\beta_1 \ln \ln Q^2/\Lambda^2}{\beta_0^2 \ln Q^2/\Lambda^2} \right) \quad (1.30)$$

where $\alpha_s^0(Q^2)$ is given by Eq. (1.7) and as calculated by Caswell and Jones [9]

$$\beta_1 = 102 - \frac{38}{3} N_f \quad (1.31)$$

Using Eqs. (1.29) and (1.30), one finds

$$M_3(N, Q^2) = \frac{K_N}{(\ln Q^2/\Lambda^2)^{d_N}} \left[1 + \frac{A_N + B_N \ln \ln Q^2/\Lambda^2}{\ln Q^2/\Lambda^2} \right] \quad (1.32)$$

with

$$B_N = - \frac{\beta_1 \gamma_0^N}{2\beta_0^3} \quad (1.33)$$

The constant A_N has been computed, although there is an ambiguity in determining A_N which results from basic ambiguities in the definitions of α_s and Λ in QCD as has been discussed by Bardeen *et al.* [10]. First,

α_s can only be defined in the context of a given renormalization scheme. In two different schemes, the definitions of the two parameters α_s disagree at second-order and are related by

$$\alpha'_s = \alpha_s + \alpha_s^2 f + \dots \quad (1.34)$$

where f is a constant depending on the definition of α'_s . Therefore, one finds that to a given order in α_s^0 the value of $\alpha_s(Q^2)$ (which is not a physical quantity) is not unique. In fact, in second-order calculations the value of $\alpha_s(Q^2 = 10 \text{ GeV}^2)$ can vary by a factor of two in different schemes which are consistent with the data. However, even if the renormalization scheme is fixed, there is still an arbitrariness in the definition of Λ which results in an ambiguity exactly like Eq. (1.34). Consider some function expanded in powers of $1/\ln Q^2$

$$F = \frac{A}{\ln Q^2/\Lambda^2} + \frac{B}{\ln^2 Q^2/\Lambda^2} + \dots \quad (1.35)$$

Now define

$$\Lambda_\rho = \Lambda e^{\frac{1}{2}\rho} \quad (1.36)$$

Then,

$$\frac{1}{\ln Q^2/\Lambda^2} = \frac{1}{\ln Q^2/\Lambda_\rho^2} - \frac{\rho}{\ln^2 Q^2/\Lambda_\rho^2} + \dots \quad (1.37)$$

and we can write

$$F = \frac{A}{\ln Q^2/\Lambda_\rho^2} + \frac{B-\rho}{\ln^2 Q^2/\Lambda_\rho^2} + \dots \quad (1.38)$$

Thus, we have the possibility of expanding using different Λ 's and getting different values of the constant in the second-order term.

If we use the definition of Λ_ρ in Eq. (1.36) for the moments of Eq. (1.32), we find

$$M_3(N, Q^2) = \frac{K_N}{(\ln Q^2/\Lambda_\rho^2)^{d_N}} \left[1 + \frac{A'_N + B_N \ln \ln Q^2/\Lambda_\rho^2}{\ln Q^2/\Lambda_\rho^2} \right] \quad (1.39)$$

where $A'_N = A_N - \rho d_N$. Note therefore, that one cannot define Λ without specifying the constant term in the second-order correction nor can one say how large the second-order term is without stating what definition of Λ is being used. Furthermore, it follows [16] that in leading-order calculations there is no clear definition of Λ ; it is not informative to quote leading-order values of Λ . In addition, leading-order results which are very sensitive to the value of Λ are likely to have significant higher-order corrections. We should point out that in comparing values of Λ or α_s from different processes, one must be sure that the same definitions of these parameters are being used. This can only be done if the second-order corrections are known. In particular, there is no meaning to comparisons of Λ 's obtained from different processes using the lowest-order results of QCD.

If one obtains the values of Λ_a and Λ_b from schemes a and b by fitting the moments for each scheme to data, one does not necessarily find that Λ_a and Λ_b are precisely related by Eq. (1.36). The variation from relation (1.36) results from the fact that different renormalization schemes have left different and significant amounts to order $(\alpha_s^0)^2$ corrections. The effects of second-order QCD corrections on fits to the moments of $x F_3$ are discussed in Section IV.

II. REVIEW OF QCD RESULTS

The QCD predictions discussed in the introduction are derived in this section using the operator-product expansion and renormalization group formalism.

A. The Operator Product Expansion

Because of asymptotic freedom, certain quantities which do not depend on the distinction between quark and hadron final states can be calculated perturbatively in QCD when all the relevant invariant masses are large [1]. However, the quantity $W_{\mu\nu}$ (see Eq. (1.2)) measured in deep-inelastic scattering satisfies neither of these requirements.

First, since $W_{\mu\nu}$ is a nucleon matrix element it certainly distinguishes between nucleon and quark states. Second, although Q^2 and $p \cdot q$ can be made large, the invariant mass p^2 is fixed by the condition $p^2 = m_p^2$.

The solution to this dilemma is the operator-product expansion [5].

The operator-product expansion expresses the product of two currents $J_\mu(x) J_\nu(0)$ as a sum of terms which are products of a c-number function of x_μ times a local operator evaluated at $x_\mu = 0$. When nucleon matrix elements are taken and the Fourier transform over x_μ is performed, each of these terms factorizes into a product of a function of Q^2 , known as a Wilson coefficient; and a target-dependent matrix element of the local operator, which does not depend on Q^2 . The Wilson coefficients are independent of p_μ and do not depend on what states are used to evaluate matrix elements. They thus satisfy all of the conditions appropriate to asymptotic freedom and can be calculated perturbatively in QCD using renormalization group methods. These calculable coefficients can be isolated by taking moments [4] of the appropriate structure function, in our case F_3 .

Rather than working directly with $W_{\mu\nu}$, we will consider $T_{\mu\nu}$ which is related to the forward Compton scattering amplitude and is defined as the Fourier transform of the spin-averaged nucleon matrix element of the time-ordered product $T\{J_{\mu}^{\dagger} J_{\nu}\}$ by

$$T_{\mu\nu} = i \int d^4z e^{iq \cdot z} \langle \vec{p} | T\{J_{\mu}^{\dagger}(z) J_{\nu}(0)\} | \vec{p} \rangle_{\text{spin averaged}} \quad (2.1)$$

From now on we will use the letter z to denote space-time coordinates to avoid confusion with the Bjorken scaling variable x . $W_{\mu\nu}$ is related to $T_{\mu\nu}$ by

$$W_{\mu\nu} = \frac{1}{\pi} \text{Im}(T_{\mu\nu}) \quad (2.2)$$

We can isolate a quantity T_3 analogous to the F_3 structure function which we wish to evaluate by writing

$$\epsilon_{\mu\nu\alpha\beta} T_{\mu\nu} = \frac{-i}{p \cdot q} (p_{\alpha} q_{\beta} - p_{\beta} q_{\alpha}) T_3 \quad (2.3)$$

Then, comparing Eqs. (1.3) and (2.3) and using (2.2) we see that

$$F_3 = \frac{1}{\pi} \text{Im}(T_3) \quad (2.4)$$

The operator product expansion relevant to T_3 is [5,6]

$$\epsilon_{\mu\nu\alpha\beta} T\{J_{\mu}^{\dagger}(z) J_{\nu}(0)\} = (g_{\alpha a} g_{\beta b} - g_{\alpha b} g_{\beta a}) \frac{\partial}{\partial z_b} \sum_i \sum_n \tilde{C}_i^n(z^2) z_{\mu_2} \dots z_{\mu_n} \mathcal{O}_i^{a\mu_2 \dots \mu_n}(0) \quad (2.5)$$

where the $\tilde{C}_i^n(z^2)$ are c-number functions, the $\mathcal{O}_i^{a\mu_2 \dots \mu_n}$ are local operators and the sums extend over all local operators with the appropriate quantum numbers to contribute to the product of currents J_{μ} .

The operator $\mathcal{O}_i^{a\mu_2 \dots \mu_n}$ is taken to have definite spin n so that the sum over n is a sum over spins while the sum over i includes all other quantum numbers required to label the local operators (such as flavor).

In order to see what Eq. (2.5) implies for the function T_3 we define the Fourier transform

$$\begin{aligned} & \int d^4z e^{iq \cdot z} \frac{\partial}{\partial z_b} \tilde{C}_i^n(z^2) z_{\mu_2} \dots z_{\mu_n} \\ &= -iq_b q_{\mu_2} \dots q_{\mu_n} \left[\frac{2^{n+1}}{(Q^2)^n} \right] C_i^n(Q^2) \end{aligned} \quad (2.6)$$

The factor in brackets is inserted for later convenience. Simple dimensional counting shows that if the operator $\mathcal{O}_i^{a\mu_2 \dots \mu_n}$ has canonical mass-dimension d_{in} then

$$C_i^n(Q^2) \propto \left(\frac{1}{Q^2} \right)^{\tau_{in}} \quad (2.7)$$

where

$$\tau_{in} = d_{in} - n \quad (2.8)$$

is called the twist of the operator $\mathcal{O}_i^{a\mu_2 \dots \mu_n}$. In an interacting quantum field theory this simple dimensional analysis does not apply because an extra mass parameter, the renormalization mass μ , appears. As a result, in general we have no reason to believe that Eq. (2.7) is correct. However, in QCD the results of Eq. (2.7) are only modified asymptotically by powers of logarithms of Q^2 so one can still argue that the leading terms in the operator product expansion when Q^2 is large come from the local operators of lowest possible twist. For T_3 these are the twist 2 operators

$$\mathcal{O}_i^{a\mu_2 \dots \mu_n} = \frac{i^{n-1}}{n!} \left[\bar{\psi} \frac{1}{2} \lambda_i \gamma_a D_{\mu_2} \dots D_{\mu_n} \psi + \text{permutations} \right] \quad (2.9)$$

where ψ is the quark field, D_μ is the gauge covariant derivative of QCD and λ_i are the generators of the flavor symmetry group $SU(N_f)$.

From now on we will restrict our discussion to leading-twist operators. Note, however, that the presence of operators of twist 4,6,8... in Eq. (2.5) implies through Eq. (2.7) that there will be corrections of order $1/Q^2$, $1/Q^4$, $1/Q^6$, ... to the basic QCD predictions. These are the higher-twist corrections discussed in the introduction.

We have chosen to arrange the operator-product expansion so that the operators $\mathcal{O}_i^{a\mu_2 \dots \mu_n}$ have definite spin n . Then the nucleon matrix elements of the $\mathcal{O}_i^{a\mu_2 \dots \mu_n}$ must be proportional to symmetric, traceless tensors of rank n , so we can write

$$\begin{aligned} \langle \vec{p} | \mathcal{O}_i^{a\mu_2 \dots \mu_n} | \vec{p} \rangle_{\text{spin averaged}} &= G_i^n \left[p_a p_{\mu_2} \dots p_{\mu_n} \right. \\ &\quad \left. - \frac{m_p^2}{4} g_{a\mu_2} p_{\mu_3} \dots p_{\mu_n} - \text{all other traces} \right] \quad (2.10) \end{aligned}$$

where the G_i^n are constants. Combining Eqs. (2.5), (2.6) and (2.10) we find

$$\begin{aligned} \epsilon_{\mu\nu\alpha\beta} T_{\mu\nu} &= -i(p_\alpha q_\beta - p_\beta q_\alpha) \sum_i \sum_n^{(\tau=2)} \left[C_i^n(Q^2) G_i^n 4 \frac{(2p \cdot q)^{n-1}}{(Q^2)^n} \right] \\ &\quad + \mathcal{O}\left(\frac{m_p^2 x^2}{Q^2}\right) + \mathcal{O}\left(\frac{1}{Q^2}\right) \quad (2.11) \end{aligned}$$

The terms marked $\mathcal{O}(m_p^2 x^2/Q^2)$ come from the trace terms in Eq. (2.10) while those marked $\mathcal{O}(1/Q^2)$ (with a mass scale set by hadronic matrix

elements) come from the higher-twist terms left out of the sum over twist 2 operators in Eq. (2.11). Because of $SU(N_f)$ symmetry in QCD all the $C_i^n(Q^2)$ with different flavor indices i will be equal and we can define

$$C_i^n(Q^2) \equiv C_n(Q^2) \quad (2.12)$$

for the twist 2 terms. It is also convenient to write

$$\sum_i G_i^n = G_n \quad (2.13)$$

again for twist 2 matrix elements. Then comparing Eq. (2.3) with Eq. (2.11) we see that

$$T_3 = 2 \sum_n \left[C_n(Q^2) G_n \left(\frac{1}{x}\right)^n \right] + \mathcal{O}\left(\frac{m^2 x^2}{Q^2}\right) + \mathcal{O}\left(\frac{1}{Q^2}\right) \quad (2.14)$$

We now relate the various terms in Eq. (2.14) to moments of F_3 . This is done by noting that T_3 is analytic in x except for a cut from $x = -1$ to $x = 1$. Thus, from Eq. (2.14) we can write

$$\frac{1}{2\pi i} \oint dx x^{N-1} T_3 = 2C_N(Q^2) G_N = \frac{1}{\pi} \int_{-1}^1 dx x^{N-1} \text{Im}(T_3) \quad (2.15)$$

Now T_3 has the crossing property $T_3(-x) = T_3(x)$ so from Eq. (2.4) we find

$$\frac{1}{\pi} \int_{-1}^1 dx x^{N-1} \text{Im}(T_3) = 2 \int_0^1 dx x^{N-1} F_3 \quad (N \text{ odd}) \quad (2.16)$$

Thus, combining Eqs. (2.15) and (2.16) we have

$$M_3(N, Q^2) = \int_0^1 dx x^{N-2} x F_3 = C_N(Q^2) G_N + \mathcal{O}\left(\frac{m^2 x^2}{Q^2}\right) + \mathcal{O}\left(\frac{1}{Q^2}\right) \quad (N \text{ odd}) \quad (2.17)$$

Actually the $\mathcal{O}(m_p^2 x^2/Q^2)$ terms can be included [6,7] in the derivation by keeping track of the trace terms in Eq. (2.10). The derivation is quite involved but leads to the result [6]

$$\tilde{M}_3(N, Q^2) = C_N(Q^2) G_N + \mathcal{O}(1/Q^2) \quad (N \text{ odd}) \quad (2.18)$$

where $\tilde{M}_3(N, Q^2)$ are the Nachtmann moments defined in Eq. (1.26). Note that the higher-twist terms of $\mathcal{O}(1/Q^2)$ appear in both (2.17) and (2.18).

Equations (2.17) and (2.18) express the results of the operator-product expansion. Although we have the restriction N odd, predictions for even N can be obtained by analytic continuation¹. We therefore will consider the QCD predictions for even and odd moments on equal footing.

B. The Renormalization Group Equations

From Eqs. (2.17) and (2.18) we see that to leading order in $1/Q^2$, the Q^2 dependence of the moments of F_3 is given by the Q^2 dependence of the Wilson coefficients $C_N(Q^2)$. This can be computed by using the renormalization group equations [18]. In a renormalizable field theory like QCD, there is an inherent arbitrariness in the definitions of renormalized coupling constants and in the renormalization of operators. In addition, when the renormalization program is carried out an arbitrary mass scale, the renormalization mass μ^2 , enters into the theory. This arbitrariness must cancel in such a way that the theory is invariant to changes in the renormalization mass when they are compensated by redefinitions of the coupling constant and renormalizations of the operators of the theory.

Because the $C_N(Q^2)$ in Eqs. (2.17) and (2.18) are dimensionless we must be able to write

$$C_N(Q^2) = C_N\left(\frac{Q^2}{\mu}, g\right) \quad (2.19)$$

where we have explicitly shown the dependence of the C_N on the QCD coupling parameter g . Now the renormalization group invariance discussed above implies that $C_N(Q^2/\mu^2, g)$ must satisfy the equation [19]

$$\left[\mu \frac{\partial}{\partial \mu} + \beta(g) \frac{\partial}{\partial g} - \gamma_N(g) \right] C_N\left(\frac{Q^2}{\mu^2}, g\right) = 0 \quad (2.20)$$

$\beta(g)$ expresses how the coupling constant g changes when μ^2 is varied and $\gamma_N(g)$ expresses the change in the normalization of the operator $\mathcal{O}_i^{a\mu_2 \dots \mu_n}$ when μ^2 is changed. The solution to Eq. (2.20) is

$$C_N\left(\frac{Q^2}{\mu^2}, g\right) = C_N\left(1, \bar{g}\left(\frac{Q^2}{\mu^2}\right)\right) \exp\left[- \int_{\bar{g}}^{\bar{g}(Q^2/\mu^2)} dg' \frac{\gamma_N(g')}{\beta(g')}\right] \quad (2.21)$$

where $\bar{g}(Q^2/\mu^2)$ is the solution to the equation

$$\mu \frac{\partial}{\partial \mu} \bar{g}\left(\frac{Q^2}{\mu^2}\right) = \beta\left(\bar{g}\left(\frac{Q^2}{\mu^2}\right)\right) \quad (2.22)$$

with the boundary condition $\bar{g}(1) = g$.

A number of interesting Q^2 dependences can be derived from Eq. (2.21) on quite general grounds. For example, in a hypothetical super-renormalizable field theory the anomalous dimensions γ_N vanish and $\bar{g} = g$. Then, from Eq. (2.21) we find $C_N(Q^2/\mu^2, g) = C_N(1, g)$ so that in this type of theory, moments of F_3 , $M_3(N, Q^2) = G_N C_N$, would scale perfectly, at least to leading order in $1/Q^2$. Another behavior which \bar{g} could exhibit

is the fixed-point behavior $\bar{g}(Q^2/\mu^2) \xrightarrow{Q^2 \rightarrow \infty} \bar{g}_f$. In this case we can write the integral in Eq. (2.21) using Eq. (2.22) as

$$\begin{aligned} \int_{\bar{g}}^{\bar{g}(Q^2/\mu^2)} dg' \left(\frac{\gamma_N(g')}{\beta_N(g')} \right) &= -\frac{1}{2} \int_0^{\ell_n Q^2/\mu^2} d \left(\ell_n \frac{Q^2}{\mu^2} \right) \gamma_N \left(\bar{g} \left(\frac{Q^2}{\mu^2} \right) \right) \\ &= -\frac{1}{2} \gamma_N(\bar{g}_f) \ell_n \frac{Q^2}{\mu^2} . \end{aligned} \quad (2.23)$$

Thus, in the fixed-point case we have

$$C_N \left(\frac{Q^2}{\mu^2}, g \right) = C_N(1, \bar{g}_f) \left(\frac{\mu^2}{Q^2} \right)^{\frac{1}{2} \gamma_N(\bar{g}_f)} \quad (2.24)$$

so that the moments $M_3(N, Q^2)$ would exhibit scaling violation by powers of Q^2 ,

$$M_3(N, Q^2) = \frac{K_N}{(Q^2)^{\frac{1}{2} \gamma_N(\bar{g}_f)}} . \quad (2.25)$$

Finally, we turn to QCD where, because of asymptotic freedom the various functions appearing in Eq. (2.21) can be calculated perturbatively. We write

$$\beta(g) = -\beta_0 \frac{g^3}{16\pi^2} - \beta_1 \frac{g^5}{(16\pi^2)^2} + \dots \quad (2.26)$$

$$\gamma_N(g) = \gamma_0^N \frac{g^2}{16\pi^2} + \gamma_1^N \left(\frac{g^2}{16\pi^2} \right)^2 + \dots \quad (2.27)$$

and

$$C_N(1, g) = 1 + \epsilon_N \frac{g^2}{16\pi^2} + \dots \quad (2.28)$$

From these expansions and Eqs. (2.21) and (2.22), the second-order expansion for the moments, Eq. (1.29), and for the coupling constant α_s , Eq. (1.30), can easily be derived [9,10]. The constant A_N in Eq. (1.29) is then given by

$$A_N = \frac{\epsilon_N}{\beta_0} + \frac{\gamma_1^N}{2\beta_0^2} - \frac{\gamma_0^N \beta_1}{2\beta_0^3} \quad (2.29)$$

For simplicity, we will only discuss the lowest-order results [1] of Eqs. (1.16) and (1.7). Substituting the lowest-order terms from Eqs. (2.26)-(2.28) into Eq. (2.21) we have

$$C_N\left(\frac{Q^2}{\mu^2}, g\right) = \exp\left[\int_g^{\bar{g}(Q^2/\mu^2)} dg' \frac{\gamma_0^N}{\beta_0 g'}\right] = \left(\frac{\bar{g}(Q^2/\mu^2)}{g}\right)^{\gamma_0^N/\beta_0} \quad (2.30)$$

Now, we turn to Eq. (2.22) which to lowest-order is just

$$\mu \frac{\partial}{\partial \mu} \bar{g}\left(\frac{Q^2}{\mu^2}\right) = -\frac{\beta_0}{16\pi^2} \bar{g}^3\left(\frac{Q^2}{\mu^2}\right) \quad (2.31)$$

with the solution

$$\bar{g}^2\left(\frac{Q^2}{\mu^2}\right) = \frac{g^2}{1 + \frac{g^2}{16\pi^2} \beta_0 \ln \frac{Q^2}{\mu^2}} \quad (2.32)$$

It is customary to define

$$\Lambda^2 = \mu^2 e^{-16\pi^2/g^2 \beta_0} \quad (2.33)$$

so that Eq. (2.32) takes the simple form

$$\bar{g}^2\left(\frac{Q^2}{\mu^2}\right) = \frac{16\pi^2}{\beta_0 \ln \frac{Q^2}{\Lambda^2}} \quad (2.34)$$

Using the definition $\alpha_s(Q^2) = \frac{g^2(Q^2/\mu^2)}{4\pi}$ we recover Eq. (1.7) of the introduction. Similarly, substituting Eq. (2.34) into Eq. (2.30) and using the relation between moments and Wilson coefficients we find the prediction of Eq. (1.16) for logarithmic scaling violations in QCD.

Finally, we note that the evolution equation of QCD, Eq. (1.6), can be derived from the above discussion by noting that the moment relation

$$M_3(N, Q^2) = \int_0^1 dx x^{N-2} (xF_3(x, Q^2)) \quad (2.35)$$

can be inverted by writing

$$xF_3(x, Q^2) = \frac{1}{2\pi i} \int_{-i\infty}^{i\infty} dN x^{1-N} M_3(N, Q^2) \quad (2.36)$$

The evolution equation can also be obtained directly by calculating radiative corrections to the quark scattering processes in leading-logarithm approximation [3].

III. ASPECTS OF A QUANTITATIVE ANALYSIS

A. Choice of Q^2 Cutoff

The QCD calculations which we are considering are perturbation expansions in α_s ($\propto 1/\ln Q^2/\Lambda^2$) and in $1/Q^2$, and are not justifiable if Q^2 is too small. Therefore, a primary problem in testing QCD in deep-inelastic scattering is the question of what lower bound on Q^2 should be used in any analysis. While it has been commonplace to set the lower limit at $Q^2 = 1$ or 2 GeV^2 , we feel the limit should be higher. Considerations of the value of α_s or of second-order corrections to the moments [9,10] may be relevant but are clouded by the arbitrariness in defining α_s and Λ (see Section IV-E). However, it is clear that terms of order $1/Q^2$ make substantial contributions in the $Q^2 = 1-3 \text{ GeV}^2$ region. A comparison of the ordinary moments, Eq. (1.10), and the Nachtmann moments, Eq. (1.26), as shown in Fig. 6 (using BEBC-Gargamelle data [12]) reveals large target-mass corrections for $Q^2 < 3 \text{ GeV}^2$ (see also Fig. 4). Furthermore, elastic scattering (a term of order $1/Q^8$) accounts for more than half of the $N=4$ moment at $Q^2 = 1$ and almost a third of it at $Q^2 = 2$ (see Fig. 7). It seems likely then that higher-twist effects as well as target-mass corrections are very important in this low Q^2 region. In other analyses it has been assumed that after target-mass corrections have been made, the remaining order $1/Q^2$ effects are small; in this case, fits of QCD to data at low Q^2 become tests of this conjecture rather than tests of QCD itself. We believe that only data with $Q^2 > 3 \text{ GeV}^2$ should be used for testing QCD. As we will show in Section IV, even for $Q^2 > 3 \text{ GeV}^2$ higher-twist terms of modest size could significantly affect ones conclusions about QCD in present data.

Clearly, one may wish to consider smaller values of Q^2 when examining questions of the contributions of $1/Q^2$ terms.

B. Other Sources of Q^2 Dependence

There are additional sources of Q^2 dependence which could conceivably affect ones conclusions about scaling violation. Since the highest Q^2 values are a reasonable fraction of the W-boson mass, propagator effects are non-zero. However, from $Q^2 = 4$ to 100 GeV^2 the resulting scaling violation is only 4% (independent of N or x) whereas QCD scaling violations are 30%-80% (depending on the particular moment).

Heavy flavor thresholds can also induce Q^2 -dependence into the structure functions. First, heavy quarks can be produced, but this is suppressed to the 5% level or less by the small mixing angles of these heavy quarks to the u and d quarks. A more important effect comes from virtual heavy quarks. For example, to lowest-order the β function is $\beta_0 = 11 - \frac{2}{3}N_f$. With heavy quark thresholds the effective number of flavors N_f is Q^2 -dependent and is given approximately by [20]

$$N_f = 3 + \frac{1}{1 + \frac{5m_c^2}{Q^2}} + \frac{1}{1 + \frac{5m_b^2}{Q^2}} . \quad (3.1)$$

From $Q^2 = 4$ to 100 GeV^2 , N_f changes from 3.3 to 4.4 and induces an additional scaling violation of about 10%. When data are fit using Eq. (3.1) rather than $N_f = 4$, one obtains a value of Λ which is about 30% smaller. It is quite unlikely that neutrino data available now or in the near future could distinguish such forms of scaling violation from logarithmic scaling violation.

C. Analysis of Data

There are two sets of data for xF_3 which we have analyzed. The BEBC-Gargamelle (BG) data [12] cover a large range of Q^2 , but the statistics are poor except for small Q^2 . For almost all Q^2 , BG data cover the entire x range. The CERN-Dortmund-Heidelberg-Saclay (CDHS) data [21] are concentrated at high Q^2 and have better statistics. However, for most Q^2 values, the x range of these data is very limited. The CDHS experimentalists made analyses [21] combining their data with SLAC eN data; we believe it is best not to do this.

Given the nature of these two sets of data, we feel it is logical to use the BG data for analyses of moments (Eq. (1.16)) and to use the CDHS data for analyses of the evolution of xF_3 (Eq. (1.6)). We have analyzed each data set by both methods, but will restrict our discussion in this paper as described above. One might consider the possibility of combining these two data sets. This idea turns out to be unwise, since the data are not consistent when both Q^2 and x are large. Consider the xF_3 data in the following bins²:

	$Q^2 = 20$ ($x = .55$ $x = .65$)	$Q^2 = 63$ ($x = .55$ $x = .65$)
CDHS	.29 ± .06 .11 ± .06	.18 ± .03 .08 ± .02
BG	.16 ± .09 .02 ± .08	.10 ± .06 .04 ± .02

For almost all other Q^2 and x values where the two data sets overlap, the BG and CDHS data are entirely consistent. However, we find contradictory results from moment analysis if the data sets are combined, because the moments give extra weight to the large x region.

For both the Q^2 -evolution and the moment approaches, we obtain the values of the free parameters by finding the minimum of the usual χ^2 function:

$$\chi^2 \equiv \frac{\sum_i \left[f_i(\text{theory}) - f_i(\text{experiment}) \right]^2}{\sum_i \sigma_i^2} \quad (3.2)$$

where the sums are over all data points (or bins) and the σ_i refer to one standard deviation uncertainties. Interpretation of the value of χ^2 involves the number of degrees of freedom (d.o.f.). The number of d.o.f. is the number of data points minus the number of free parameters. By statistical analysis, one expects χ^2 to be approximately 1 per d.o.f. for a good fit; clearly χ^2 increases for poor fits. In analyzing the BG and CDHS data and comparing with QCD predictions, we obtain the puzzling results that in general χ^2 is less than 1 per d.o.f. (ranging from about 0.5 to 0.8). Low χ^2 are statistically unlikely. This problem may result from overestimates of uncertainties. In some cases we rescale (or renormalize) the value of χ^2 in the QCD case to 1 per d.o.f. in order to judge the relative probabilities of alternatives to QCD. In other words, we multiply the χ^2 values of QCD and of alternatives by a common factor. Clearly such a procedure has serious drawbacks, and no important conclusions should or will be based on it.

Standard deviations for each parameter are obtained as follows: Parameter x_1 is varied away from its fitted value. For each new value of x_1 , the other parameters are varied to obtain the best χ^2 . This is repeated until a value of x_1 is obtained for which its best χ^2 is 1.0 greater than the χ^2 for the original fitted x_1 . The same procedure is followed for parameters x_2 , x_3 , etc.

In fitting the BG data we consider the $N=2,3,4,5$ and 6 moments of xF_3 (moments with $N \geq 7$ would measure the same large x bins again). Since BG had no acceptance and therefore no data in the $Q^2 = 64 \text{ GeV}^2$, $x = 0.05$ bin, we extrapolate the data and add a 100% error ($xF_3 = 1.1 \pm 1.1$). Previous analyses have used $xF_3 = 0 \pm 0$, but we feel our procedure is more reasonable. To obtain the best fit (and minimize χ^2), the coefficients $K_2 - K_6$ (see Eq. (1.16)) and Λ are all varied simultaneously.

It is also of interest to find ratios of anomalous dimensions which can be done by finding the slope when $\ln M_3(N_1, Q^2)$ is plotted versus $\ln M_3(N_2, Q^2)$ [12]. However, in this case, special care must be taken, because there are very strong correlations in the uncertainties for $M_3(N_1, Q^2)$ and $M_3(N_2, Q^2)$ (especially if $N_1 = N_2 + 1$); these correlations occur because each moment is an integral over xF_3 . In our analysis, σ_i in Eq. (3.2) was modified to account for these correlations.

In fitting the CDHS data using the Q^2 -evolution equation (Eq. (1.6)), we assume the form $F(x, Q_0^2) = Cx^a(1-x)^b$. This form is entirely consistent with the neutrino data, so there would be little value in using a form with additional parameters. We choose Q_0^2 to be 152.4 GeV^2 (the highest CDHS data point) and then evolve to lower Q^2 ; note that $xF_3(x, Q_0^2) \approx F(x, Q_0)$ for such large Q_0^2 , see Eq. (1.21). The parameters a and b describe the parameterization at $Q^2 = Q_0^2$. With each variation of a and b , we use Eqs. (1.21) and (1.23) to calculate xF_3 in all other x and Q^2 bins and then compare with the data to obtain χ^2 . In this way we obtain the parameters a, b and Λ simultaneously using the data at all Q^2 values. Our results are almost totally independent of which values we choose for Q_0^2 (although different values of a and b are obtained, of course).

The value of the constant C in $Cx^a(1-x)^b$ is obtained using the Gross-Llewellyn-Smith sum rule [22]. This sum rule requires that the $N=1$ moment be equal to 3 in leading order (where this entire calculation is done). Using $x\mathcal{F}_3 = Cx^a(1-x)^b$, this results in

$$C = \frac{3\Gamma(a+b+1)}{\Gamma(a)\Gamma(b+1)} \quad (3.3)$$

We have also allowed C to be the fourth free parameter; this procedure results in somewhat different values for a and b , but it gives almost identically the same value for Λ and does not affect any of our conclusions.

IV. ON THE COMPARISON OF THEORY WITH EXPERIMENT

In this section we address several questions concerning the presence and form of scaling violations, the role of anomalous dimensions and the effect of different renormalization schemes. All of these questions center on the problem of testing QCD. Can the present data be taken as evidence for the validity of QCD? What are the appropriate methods and considerations in testing QCD?

There is no question that scaling violation does exist in some form. Using the BEBC-Gargamelle (BG) data [12], one finds that the probability of perfect scaling ($M_3(N, Q^2) = K_N \equiv \text{constants}$) is only 1 in 10^3 for $Q^2 > 3 \text{ GeV}^2$ and much smaller if data for $Q^2 > 1 \text{ GeV}^2$ are used.

For each question we raise, we will consider answers in the contexts of both moment analysis, Eq. (1.26), and Q^2 -evolution, Eqs. (1.21)-(1.23). In the analyses which follow we will always use Nachtmann moments, but no qualitative conclusions would be changed by using ordinary moments. Since we use only high Q^2 data for the Q^2 -evolution approach, the differences between use of x -scaling and ξ -scaling are negligible.

A. Is QCD Consistent with Present Data?

Our analysis (like earlier analyses [10,12,21,23,24]) finds that the present data are entirely consistent with the predictions of QCD. In the moment analysis, somewhat different values for the parameters (λ, K_N) are obtained using second-order (in α_s) calculations [9,10], but the resulting curves are almost identical to the leading-order curves and the quality of the fit is therefore almost identical for the two

cases. QCD fits to the data are excellent even down to $Q^2 = 1 \text{ GeV}^2$ (see Figs. 8 and 9). As discussed in Section III-C, the χ^2 obtained are, in fact, smaller than would ordinarily be expected from statistical analyses. This is shown in Table I. Recall that we require $Q^2 > 3$ for testing QCD; for consideration of the effects of $1/Q^2$ corrections we allow lower Q^2 values.

The χ^2 for QCD are consistently as low as the χ^2 we have obtained for any fits. As a consequence we have chosen to use QCD as a standard for comparison with other results. We obtain relative probabilities following the procedure of Section III-C. By virtue of this procedure, the relative probabilities for QCD are always defined as 50%.

While QCD is unquestionably consistent with the scaling violation observed in present data, there are other sources of Q^2 dependence which may also be important. We now address this question.

B. Could All Scaling Violation Come From Higher-Twist Terms?

In any theory one expects corrections from higher-twist terms. It is informative, therefore, to inquire as to whether these terms might account for all or a substantial portion of the observed scaling violation.

We must assume a form for the higher-twist terms. For the moments we assume (following Eq. (1.28)) either one or two additional terms:

$$M_3(N, Q^2) = K_N \left(1 + \frac{aN}{Q^2} \right) \quad (4.1)$$

or

$$M_3(N, Q^2) = K_N \left(1 + \frac{aN}{Q^2} + \frac{bN^2}{Q^4} \right) \quad (4.2)$$

where the K_N are again free parameters. Our results are shown in Table

Table I

The χ^2 for QCD and the degrees of freedom (d.o.f.) obtained using Eqs. (1.16) or (1.32) for $M_3(N, Q^2)$ and Eqs. (1.21) - (1.23) for $xF_3(x, Q^2)$. Data are from Refs. [12] and [21].

Data	Quantity Tested	χ^2	d.o.f.	$\chi^2/\text{d.o.f.}$
BG ($Q^2 > 3$)	$M_3(N, Q^2)$	10.9	14	0.78
BG ($Q^2 > 1$)	$M_3(N, Q^2)$	20	29	0.69
CDHS ($Q^2 > 3$)	$xF_3(x, Q^2)$	19	42	0.45

II. They indicate that order $1/Q^2$ terms with coefficients of order 1 GeV^2 could account for the observed scaling violation; this is also clear in Fig. 8. Since coefficients of this size are difficult to rule out on theoretical grounds, we see that higher-twist effects can have a large impact on QCD analyses.

For study of higher-twist contributions using xF_3 , we assume (following Eq. (1.27)) that xF_3 can be parameterized in one of the following two forms:

$$xF_3(x, Q^2) = c \left[x^a (1-x)^b + d \sqrt{x} (1-x)^2 / Q^2 \right] \quad (4.3)$$

or

$$xF_3(x, Q^2) = c \left[x^a (1-x)^b + d \sqrt{x} (1-x)^2 / Q^2 + e \sqrt{x} (1-x) / Q^4 \right] \quad (4.4)$$

Our results are shown in Table III and Fig. 9. Again order $1/Q^2$ terms could account for most or all of the scaling violation.

We are not necessarily suggesting that higher-twist terms alone account for the observed scaling violation, but these results do suggest that their impact on analyses of scaling violation could be substantial.

The question arises whether the data could separate the scaling violation of QCD from the scaling violation of higher-twist terms. We have used two methods to investigate this question. We assumed the following form for $M_3(N, Q^2)$:

$$M_3(N, Q^2) = \frac{K_N}{(\ln Q^2 / \Lambda^2)^{d_N}} \left(1 + \frac{aN}{Q^2} \right) \quad (4.5)$$

In the first approach we left both a and Λ as free parameters and used data for $Q^2 > 1 \text{ GeV}^2$. We found $a = 0.12 \pm 0.90$; clearly, this is not a

Table II

The χ^2 and relative probabilities for the given forms of moments using BG data [12] with Q^2 in GeV^2 . The relative probability for QCD is 0.50 and χ^2 per d.o.f. is 0.8 ($Q^2 > 3$) and 0.7 ($Q^2 > 1$).

BG Data	Form of $M_3(N, Q^2)$	χ^2 per d.o.f.	Relative Probability	Parameters
$Q^2 > 3$	$K_N \left(1 + \frac{aN}{Q^2}\right)$	0.9	0.35	$a = 0.8 \pm 0.2$
$Q^2 > 3$	$K_N \left(1 + \frac{aN}{Q^2} + \frac{bN^2}{Q^4}\right)$	0.8	0.51	$a = 1.8 \pm 0.8$ $b = -0.8 \pm 0.6$
$Q^2 > 1$	$K_N \left(1 + \frac{aN}{Q^2}\right)$	0.9	0.16	$a = 0.8 \pm 0.1$
$Q^2 > 1$	$K_N \left(1 + \frac{aN}{Q^2} + \frac{bN^2}{Q^4}\right)$	0.9	0.12	$a = 0.6 \pm 0.2$ $b = 0.05 \pm 0.04$

Table III

The χ^2 and relative probabilities for the given forms of xF_3 using CDHS data [21] with $Q^2 > 3 \text{ GeV}^2$. The relative probability for QCD is 0.50 and χ^2 per d.o.f. is 0.45.

Form of $xF_3(x, Q^2)$	χ^2 per d.o.f.	Relative Probability	Parameters
$c \left[x^a (1-x)^b + \frac{d\sqrt{x}(1-x)^2}{Q^2} \right]$	0.57	0.13	$d = 0.4 \pm 0.2$
$c \left[x^a (1-x)^b + \frac{d\sqrt{x}(1-x)^2}{Q^2} + \frac{e\sqrt{x}(1-x)}{Q^4} \right]$	0.50	0.41	$d = 1.5 \pm 0.7$ $e = -4.0 \pm 2.0$

useful result. For the second method, it was further assumed that $aN/Q^2 \ll 1$ for $Q^2 > 3 \text{ GeV}^2$, so that the value of Λ could be determined independent of the value of a by using BG data with $Q^2 > 3$. Then holding Λ fixed at that value, the magnitude of a could be determined using all BG data with $Q^2 > 1 \text{ GeV}^2$. We found $a = 0.17 \pm 0.04$. However, there was no improvement in χ^2 , and this value of a means that aN/Q^2 is not small as was assumed above. Similar results were obtained from analysis of CDHS data. One concludes that the present data cannot separate $(\ln Q^2/\Lambda^2)^{-d_N}$ behavior from $(1 + aN/Q^2)$ behavior. It follows that the value of Λ obtained for QCD when higher-twist contributions are neglected may be absorbing the effects of these $1/Q^2$ terms.

C. Can Power-Law and Logarithmic Scaling Violations Be Distinguished?

As discussed in Section II (see Eq. (2.25)), fixed-point theories exhibit power-law scaling violation of the form $M_3(N, Q^2) \propto (Q^2)^{-b_N}$ where the numbers b_N are not determined. For discussion of these hypothetical fixed-point theories, we have chosen two quite different parameterizations of b_N . In one case we assume there is no N -dependence and in the other case we assume the N -dependence is the same as for QCD except for an overall coefficient. At first thought, it may seem that one should be able to distinguish power-law behavior from the logarithmic behavior $[(\log Q^2/\Lambda^2)^{-d_N}]$ of QCD. We have argued in Section III that tests of QCD and alternatives should use only data with $Q^2 > 3 \text{ GeV}^2$. As can be seen from the first part of Table IV, with present data for $Q^2 > 3$, it is, in fact, impossible to distinguish these two behaviors.

It is interesting to observe that while fixed-point theories are absolutely as good as QCD for $Q^2 > 3 \text{ GeV}^2$, it appears (at first glance)

Table IV

The χ^2 and relative probabilities for fixed-point theories. For xF_3 we use the evolution equation, Eq. (1.6), with $\alpha_s^0(Q^2)$ replaced by a constant which is the fixed-point coupling α_f and is assumed to be small. The units of Q^2 are GeV^2 . The relative probability for QCD is always 0.50 and χ^2 per d.o.f. are 0.8 (BG moments, $Q^2 > 3$), 0.7 (BG moments, $Q^2 > 1$) and 0.45 (CDHS, xF_3). d_N is defined in Eq. (1.15). There are virtually no CDHS data for $Q^2 < 3$. The data are from Refs. [12] and [21].

Data	Quantity Tested	$\chi^2/\text{d.o.f.}$	Relative Probability	Parameters
BG ($Q^2 > 3$)	$M_3 = K_N/(Q^2)^{C_0}$	0.82	0.45	$C_0 = 0.21 \pm 0.04$
BG ($Q^2 > 3$)	$M_3 = K_N/(Q^2)^{C_0^{dN}}$	0.76	0.51	$C_0 = 0.24 \pm 0.05$
CDHS ($Q^2 > 3$)	xF_3	0.45	0.50	$\alpha_f = 0.19 \pm 0.05$
BG ($Q^2 > 1$)	$M_3 = K_N/(Q^2)^{C_0}$	1.86	10^{-5}	$C_0 = 0.30 \pm 0.02$
BG ($Q^2 > 1$)	$M_3 = K_N/(Q^2)^{C_0^{dN}}$	1.38	0.002	$C_0 = 0.41 \pm 0.03$
BG ($Q^2 > 1$)	$M_3 = \frac{K_N}{(Q^2)^{C_0}} \left(1 + \frac{.008N}{Q^2} + \frac{.07N^2}{Q^4} \right)$	0.78	0.32	$C_0 = 0.19 \pm 0.09$

that they would be completely ruled out if data with $Q^2 > 1 \text{ GeV}^2$ were considered, as is shown in the second part of Table IV. However, note in the third part of Table IV that the addition of quite small higher-twist terms to fixed-point theories allows an excellent fit to the data even for $Q^2 > 1 \text{ GeV}^2$. The reason QCD without higher-twist terms does so well at low Q^2 is that it has a pole at low Q^2 , whereas the fixed-point predictions are finite until Q^2 equals zero. However, the QCD pole is an artifact of the perturbation expansion, and its effects cannot be considered as valid predictions of the theory. It is critical to consider the impact of higher-twist terms before arguing that data prefer QCD over other theories. Here we find that the present data do not distinguish QCD from fixed-point theories.

D. Are Anomalous Dimensions A Good Test for QCD?

From the lowest-order QCD predictions for the moments, Eq. (1.16), one sees that

$$\frac{[M_3(M, Q^2)]^{r_{NM}}}{M_3(N, Q^2)} = \text{constant} \quad (4.6)$$

for all Q^2 when $r_{NM} = d_N/d_M$. Equivalently, one can take the logarithm of Eq. (4.6) and write

$$\ln M_3(N, Q^2) = r_{NM} \ln M_3(M, Q^2) + \text{constant} \quad (4.7)$$

Thus, it has been suggested [12] that QCD can be tested by determining r_{NM} from the data using either Eq. (4.6) or Eq. (4.7) and comparing it with the QCD prediction d_N/d_M . However, this test is affected by both α_s and $1/Q^2$ corrections which can modify the basic QCD predictions.

When the second-order expressions for the moments, Eq. (1.32), are substituted into Eq. (4.6), one finds [23] that the equality can no longer be satisfied at all Q^2 . Therefore, the above test is ambiguous when these corrections are included. If one wishes, one can set

$$\frac{\partial}{\partial Q^2} \frac{[M_3(M, Q^2)]^{r_{NM}}}{M_3(N, Q^2)} = 0 \quad (4.8)$$

to determine r_{NM} as a function of Q^2 . The lowest-order QCD predictions for various N and M are shown by the horizontal lines in Fig. 10 while the shaded areas indicate the range for the second-order QCD predictions, based on the value of Q^2 and Λ used in evaluating r_{NM} . Since the prediction for r_{NM} is of the form $r_{NM} = d_N/d_M + \mathcal{O}(\alpha_s^0)$, there exists the same type of lowest-order QCD ambiguity for Λ as discussed in the introduction. Thus in this separate expansion, the Λ to be used in evaluating r_{NM} is not necessarily the same Λ as one obtains in fitting the moments. We have argued that tests of QCD should use $Q^2 > 3 \text{ GeV}^2$, however we have shown for comparison the $Q^2 > 1 \text{ GeV}^2$ values as well. Our values are different from those originally reported by the BG experimentalists [12]. We have used an improved error analysis and for one bin we use extrapolated BG data. For the $Q^2 = 63 \text{ GeV}^2$, $x = 0.05$ bin we use $x F_3 = 1.1 \pm 1.1$ instead of 0 ± 0 (see discussion in Section III). Note that QCD is in good agreement with the data for $Q^2 > 3 \text{ GeV}^2$ although the error bars on the data for these large Q^2 values are quite large.

A question which is crucial to use of anomalous dimensions as a test of QCD is: Are the results shown in Fig. 10 (which are consistent with QCD) unique predictions of QCD or are these ratios also likely to

arise from other sources. In fact, we find that the observed values of r_{NM} are very similar to those which are likely to arise from higher-twist terms. Consider a form which includes one higher-twist term but has no logarithmic or power-law $[(Q^2)^{-b_N}]$ behavior:

$$M_3(N, Q^2) = K_N \left(1 + \frac{aN}{Q^2} \right) \quad . \quad (4.9)$$

one then finds

$$r_{NM} = \frac{N}{M} \left(\frac{1 + \frac{aM}{Q^2}}{1 + \frac{aN}{Q^2}} \right) \quad (4.10a)$$

and

$$r_{NM} \approx \frac{N}{M} \quad \text{for small } \frac{a}{Q^2} \quad . \quad (4.10b)$$

The data for r_{NM} do, in fact, resemble the N/M dependence which results from Eq. (4.9). If one uses

$$M_3(N, Q^2) = K_N \left(1 + \frac{aN}{Q^2} + \frac{bN^2}{Q^4} \right) \quad (4.11)$$

then one finds that $r_{NM} \approx N/M$ as long as a and b are positive and are of order 1 GeV^2 and 1 GeV^4 (respectively) or smaller. It is evident from Eq. (4.7) that on a plot of $\ln M_3(N, Q^2)$ versus $\ln M_3(M, Q^2)$ the slope is equal to r_{NM} . In Fig. 11, we show such plots for QCD and for Eq. (4.11) (with a and b taken from the last entry in Table II). Note that the comparison of the theoretical curves with the data on this plot is misleading since the strong correlations between $M_3(N, Q^2)$ and $M_3(M, Q^2)$ (discussed in Section III-C) are not evident. The plot does show, however, that for a significant range of Q^2 the slopes (r_{NM}) predicted by QCD and by Eq. (4.11) are very similar.

We find, then, two conclusions about use of r_{NM} . First, it is likely that higher-twist contributions will not significantly affect the QCD predictions, so that $r_{NM} \approx d_N/d_M$ remains a prediction of the theory. Second, given the role of higher-twist terms, one can question whether conclusions about alternative theories with different N dependences can be believed. Among such hypothetical theories are those with scalar gluons [25] for which the anomalous dimensions change much more slowly with N than do those of QCD. The predictions for r_{NM} of such theories may be drastically altered by the presence of quite small higher-twist terms.

Given the lack of precision of second-order predictions for r_{NM} and the confusion generated by the presence of higher-twist terms, we believe that great caution should be employed in using anomalous dimensions as a test for QCD. But it must be noted that QCD (with or without higher-twist terms) is entirely consistent with the data for r_{NM} as it is with all other data discussed here.

E. Can the Data Choose the Best Definitions of α_s and Λ ?

As discussed at the end of Section I, use of second-order QCD calculations of the moments [9,10] for fitting to the data involves a choice of which definition of Λ and which value of the parameter ρ to use. Recall that $A'_N = A_N - \rho d_N$ in Eq. (1.39):

$$M_3(N, Q^2) = \frac{K_N}{(\ln Q^2/\Lambda_\rho^2)^{d_N}} \left[1 + \frac{A'_N + B_N \ln \ln Q^2/\Lambda_\rho^2}{\ln Q^2/\Lambda_\rho^2} \right]. \quad (4.12)$$

There are several possible approaches to choice of Λ and α_s . The calculations [9,10] of the A_N were done in the minimal subtraction

scheme using dimensional regularization. The A_N contain factors of $\ln(4\pi) - \gamma_E$ coming from expanding around dimension $n=4$ in the dimensional regularization method. Since these factors can be considered as artifacts of the regularization scheme, one can choose³

$$\rho = \ln(4\pi) - \gamma_E \approx 2 \quad (4.13)$$

in order to remove such factors from the A_N [10].

There is another approach to this problem which would be ideal if the data were perfect. That approach is to allow ρ to be another free parameter in the fit. This would have the result of minimizing the effects of third-order terms (and other higher-order terms) for the Q^2 range and moments of interest. Using data with $Q^2 > 3 \text{ GeV}^2$, we find $\rho = -1.6$ with a large uncertainty of about ± 10 and no improvement in χ^2 . It is interesting to note, however, that using data for $Q^2 > 1 \text{ GeV}^2$ we obtain $\rho = 2.3 \pm 0.6$ (similar to Eq. (4.13)) and χ^2 per d.o.f. is reduced from 0.7 to 0.6 (d.o.f. = 29). Given the role played by higher-twist terms it is difficult to judge the significance of this last result.

A third approach to choosing the parameter ρ lies in trying to find a theoretical justification for the assumption that a particular choice of ρ will minimize the uncalculated third-order terms (and higher-order terms) in the moments. The most apparent theoretical assumption is that if the second-order term is small, higher-order terms should also be small [23]. One finds that for the Q^2 range and moments of interest, the second-order terms are minimized by choosing $\rho \approx 2$; for $1 < Q^2 < 100 \text{ GeV}^2$ and $N=2-6$; the ratio of second- to first-order terms then averages about 0.07. It is interesting that $\rho \approx 2$ is

indicated by all three approaches.

We have remarked previously (Section I) that the value of $\alpha_s(Q^2)$ is renormalization-scheme dependent, but of course $\alpha_s(Q^2)$ is not a directly measurable quantity. With $\alpha_s(Q^2)$ defined by Eq. (1.30) for $\rho = 0$, one finds (using Eq. (1.38)) for other values of ρ that

$$\alpha_s(Q^2) = \alpha_s^0\left(\frac{Q^2}{\Lambda_\rho^2}\right) \left\{ 1 - \frac{\left[\frac{\beta_1}{\beta_0^2} \ln \ln Q^2/\Lambda_\rho^2 + \rho \right]}{\ln Q^2/\Lambda_\rho^2} \right\}. \quad (4.14)$$

$\alpha_s(Q^2)$ could have been defined by Eq. (1.30) for a value of ρ other than zero; then various formulae in this paper would be modified accordingly. However, with the present definition it is interesting to note three cases. For the first case, $\rho = 0$, we find that the second-order corrections to the moments and to $\alpha_s(Q^2)$ are about 25% of the first-order terms. For $\rho \approx -1.3$ we find that the second-order term in $\alpha_s(Q^2)$ is minimized (it is near zero), but in the moments the second-order term is about 40%. Finally for $\rho \approx 2$ we find (as discussed above) that the second-order corrections to the moments are minimized. However, the second-order term in $\alpha_s(Q^2)$ (in Eq. (4.14)) is very large (65% at $Q^2 = 10 \text{ GeV}^2$ and 100% at $Q^2 = 1 \text{ GeV}^2$).

As a result $\alpha_s(Q^2)$ is small for $\rho = 2$ only by an accident of the perturbation expansion; in fact, it goes to zero as Q^2 drops to 1 GeV^2 . The $\alpha_s(Q^2)$ curves for these three values of ρ are shown in Fig. 12. It is clear that it is not possible to quote the value of $\alpha_s(Q^2)$ (much less Λ) except in the context of particular definitions of Λ and ρ . With more precise data, it may be possible to identify the best choice for Λ and ρ (that which will minimize higher-order corrections in physical quantities).

V. CONCLUSIONS

In our analysis we found again and again that quantum chromodynamics gave as good or better fits to the data as any alternative. This was true down to $Q^2 = 1 \text{ GeV}^2$ whether or not higher-twist contributions were included. Since higher-twist contributions have not yet been calculated in QCD, it would be useful if one could estimate them from the data. Unfortunately the data at present are not precise enough to allow this estimation. When considering hypothetical alternative theories, we found that the inclusion of small higher-twist terms allowed for fits to the data almost as good as those for QCD. The inability to separate QCD from alternatives under these conditions results from a lack of sufficiently precise data at sufficiently high Q^2 (where higher-twist terms are likely to be small). The corrections of second-order in α_s do not introduce any serious problems in testing QCD. The parameters Λ and α_s are not meaningful except in second-order calculations when particular definitions have been expressed. Again more precise data at high Q^2 may suggest the most practical definitions. We have argued that tests of QCD should be done only with data for $Q^2 > 3 \text{ GeV}^2$. However, accurate low Q^2 data could still be helpful in sorting out higher-twist effects.

ACKNOWLEDGEMENTS

The authors are grateful to D. Perkins and W. Scott of the BEBC-Gargamelle collaboration and P. Bloch, D. Schlatter and J. Steinberger of the CDHS collaboration for providing us with their data and for detailed discussions of their analyses and results. We thank R. Blankenbecler, A. Buras, G. Fox, F. Gilman and D. Politzer for useful discussions. We wish to especially acknowledge the many contributions and the encouragement of S. Brodsky. This research was supported in part by the Department of Energy.

FOOTNOTES

1. When calculated to second-order in α_s , the anomalous dimensions have the general form $\gamma_N = \gamma_A^N + (-1)^N \gamma_B^N$ so that the γ_N for even N are not defined by a unique analytic continuation from those for odd N . However, the numerical difference between $\gamma_A^N - \gamma_B^N$ and $\gamma_A^N + \gamma_B^N$ for even N is quite small and this subtlety will be ignored in our phenomenological analysis. See Ref. [17] for further details.
2. CDHS results in this table are obtained by interpolating between neighboring data points.
3. In the scheme with $\rho = \ln(4\pi) - \gamma_E$ which is the \overline{MS} scheme of Ref. [10], we find $\Lambda_{\overline{MS}} = 0.287 \pm 0.148$ GeV for $Q^2 > 3$ GeV² with N_f given by Eq. (3.1).

REFERENCES

1. H. D. Politzer, Phys. Rev. Lett. 26 (1973) 1346; D. Gross and F. Wilczek, Phys. Rev. Lett. 26 (1973) 1343 and Phys. Rev. D8 (1973) 3633 and D9 (1974) 980; A. Zee, F. Wilczek and S. B. Treiman, Phys. Rev. D10 (1974) 2881; H. Georgi and H. D. Politzer, Phys. Rev. D9 (1974) 416; S. Weinberg, Phys. Rev. Lett. 31 (1973) 494. Some reviews are: H. D. Politzer, Phys. Reports 14C (1974) 129; D. J. Gross in Methods in Field Theory, ed. R. Balian and J. Zinn-Justin (North Holland, Amsterdam, 1976); J. Ellis in Weak and Electromagnetic Interactions at High Energy, ed. R. Balian and C. H. Llewellyn Smith (North Holland, Amsterdam, 1977); C. H. Llewellyn Smith, Report No. OXFORD-TP 2/78 (Lectures at the 1977 Cargese Summer Institute); O. Nachtmann in 1977 Proceedings of the International Symposium on Lepton and Photon Interactions at High Energy, ed. F. Gutbrod (DESY, Hamburg, 1977); W. J. Marciano and H. R. Pagels, Phys. Reports C36 (1978) 137; A. J. Buras, Report No. FERMILAB-PUB 79/17 THY (January 1979).
2. J. D. Bjorken and E. A. Paschos, Phys. Rev. 158 (1969) 1975; J. D. Bjorken, Phys. Rev. 179 (1969) 1547; R. P. Feynman, Photon-Hadron Interactions (Benjamin, Reading, 1972).
3. G. Altarelli and G. Parisi, Nucl. Phys. B126 (1977) 298; Yu. L. Dokshitzer, D. I. Dyakonov and S. I. Troyan, Report No. SLAC-TRANS-0183 (June 1978), translated from Proceedings of the 13th Leningrad Winter School on Elementary Particle Physics, 1978, pp. 1-89; J. Kogut and L. Susskind, Phys. Rev. D9 (1974) 697 and 3391; G. Parisi, Phys. Lett. 43B (1973) 207; D. J. Gross, Phys.

- Rev. Lett. 32 (1974) 1071; C. H. Llewellyn Smith, Report No. OXFORD-TP 47/78 (February 1978); W. R. Frazer and J. F. Gunion, Report No. UCSD-10P10-194 (October 1978).
4. J. M. Cornwall and R. E. Norton, Phys. Rev. 177 (1969) 2584.
 5. K. Wilson, Cornell Report No. LNS-64-15 (unpublished) and Phys. Rev. 179 (1969) 1499.
 6. O. Nachtmann, Nucl. Phys. B63 (1973) 237; S. Wandzura, Nucl. Phys. B122 (1977) 412.
 7. H. Georgi and H. D. Politzer, Phys. Rev. D14 (1976) 1829, and Phys. Rev. Lett. 36 (1976) 1281.
 8. R. Barbieri, J. Ellis, M. K. Gaillard and G. G. Ross, Phys. Lett. 64B (1976) 171 and Nucl. Phys. B117 (1976) 50; R. K. Ellis, R. Petronzio and G. Parisi, Phys. Lett. 64B (1976) 97.
 9. E. G. Floratos, D. A. Ross and C. T. Sachrajda, Nucl. Phys. B129 (1977) 66 (erratum - B139 (1978) 545); Report No. CERN-TH-2566 (October 1978) and Phys. Lett. 80B (1979) 269. The second-order β function was calculated by W. E. Caswell, Phys. Rev. Lett. 33 (1974) 244 and D.R.T. Jones, Nucl. Phys. B75 (1974) 531.
 10. W. A. Bardeen, A. J. Buras, D. W. Duke and T. Muta, Phys. Rev. D18 (1978) 3998; W. A. Bardeen and A. J. Buras, Report No. FERMILAB-PUB-79/31-THY (May 1979).
 11. D. J. Gross, S. B. Treiman and F. A. Wilczek, Phys. Rev. D15 (1977) 2486; K. Bitar, P. W. Johnson and W. K. Tung, Illinois Inst. of Tech. Report (December 1978); H. Georgi and H. D. Politzer, Phys. Rev. D15 (1977) 2495.

12. P. C. Bosetti et al., Nucl. Phys. B142 (1978) 1; D. Perkins, Oxford Report No. OXFORD-NP 2/79 (December 1978).
13. E. Bloom and F. Gilman, Phys. Rev. Lett. 25 (1970) 1140.
14. A. DeRújula, H. Georgi and H. D. Politzer, Phys. Lett. 64B (1977) 428 and Annals Phys. 103 (1977) 315.
15. S. Brodsky and G. Farrar, Phys. Rev. Lett. 31 (1973) 1153 and Phys. Rev. D11 (1975) 1309; R. Blankenbecler and S. Brodsky, Phys. Rev. D10 (1974) 2973.
16. M. Bace, Phys. Lett. 78B (1978) 132; S. Wolfram, Caltech Report No. CALT-68-690 (October 1978); W. Celmaster and R. J. Gonsalves, UCSD Report No. UCSD-10P10-202 (May 1979); A. N. Schellekens, Nijmegen Report No. THEF-NYM-78-8 (January 1979).
17. D. A. Ross and C. T. Sachrajda, Nucl. Phys. B149 (1979) 497.
18. M. Gell-Mann and F. Low, Phys. Rev. 95 (1954) 1300; C. Callan, Phys. Rev. D2 (1970) 1541; K. Symanzik, Commun. Math. Phys. 18 (1970) 227; S. Coleman in Properties of the Fundamental Interactions, ed. A. Zichichi (Editrice Compositori, Bologna, 1973).
19. N. Christ, B. Hasslacher and A. Mueller, Phys. Rev. D6 (1972) 3543.
20. A. DeRújula and H. Georgi, Phys. Rev. D13 (1976) 1296; E. Poggio, H. Quinn and S. Weinberg, Phys. Rev. D13 (1976) 1958.
21. J. G. H. DeGroot et al., Phys. Lett. 82B (1979) 292 and 456, and Zeit. f. Phys. C1 (1979) 142.
22. D. J. Gross and C. H. Llewellyn Smith, Nucl. Phys. B14 (1969) 337.
23. R. Barbieri, L. Caneschi, G. Curci and E. d'Emilio, Phys. Lett. 81B (1979) 207; see also H. Harari, Report No. SLAC-PUB-2254 (January 1979).

24. G. C. Fox, Nucl. Phys. B131 (1977) 107 and B134 (1978) 269; A. J. Buras and K.J.F. Gaemers, Nucl. Phys. B132 (1978) 249; L. F. Abbott, Report No. SLAC-PUB-2296 (to appear in the Proceedings of Orbis Scientiae, 1979, Coral Gables, Florida); P. W. Johnson and W. K. Tung, Nucl. Phys. B121 (1977) 270; M. Gluck and E. Reya, Report No. DESY-79/13 (February 1979); D. W. Duke and R. G. Roberts, Rutherford Report No. RL-79-025 (March 1979); L. Baulieu and C. Kounnas, Ecole Normale Report No. LPTENS 78/27 (December 1978); V. Baluni and E. Eichten, Phys. Rev. Lett. 37 (1976) 1181 and Phys. Rev. D14 (1976) 3045.
25. D. Bailin and A. Love, Nucl. Phys. B75 (1974) 159; M. Gluck and E. Reya, Phys. Rev. D16 (1977) 3242.

FIGURE CAPTIONS

- Fig. 1. Kinematics of deep-inelastic lepton scattering. q_μ labels the transferred momentum and p_μ the initial nucleon momentum.
- Fig. 2. A diagram which depends on the gluon distribution in the nucleon but which does not contribute to the F_3 structure function.
- Fig. 3. An example of a current striking a quark of momentum fraction x which arises from a quark of momentum fraction w after gluon radiation.
- Fig. 4. The solid curve is an x -scaling fit of QCD to the data of Ref. [12] while the dashed curve is the corresponding ξ -scaling prediction of QCD. Elastics are shown in an extra bin from $x=1$ to $x=1.1$ where the area under the data point in this bin is equal to the area under the elastic spike at $x=1$ in the original data. Note that a significant elastic contribution is present and that the x - and ξ -scaling curves are quite different at this value $Q^2 = 1.7 \text{ GeV}^2$.
- Fig. 5. Same as Fig. 4 except that $Q^2 = 3.9 \text{ GeV}^2$. Note that the elastics are now negligible and that the x -(solid) and ξ -(dashed) scaling curves are nearly identical.
- Fig. 6. A comparison of ordinary moments and Nachtmann moments from the data of Ref. [12]. Curves are drawn connecting the data points to help guide the eye. The two types of moments are significantly different for $Q^2 < 3 \text{ GeV}^2$ indicating large target-mass effects in this Q^2 region.

Fig. 7. Nachtmann moments computed with and without elastic scattering contributions. Curves are drawn connecting the data points to help guide the eye. Data are from Ref. [12]. The curves show a significant elastic contribution for $Q^2 < 3 \text{ GeV}^2$.

Fig. 8. Nachtmann moments for $N = 2-6$ from the data of Ref. [12]. The solid curves are the QCD predictions for these moments. The dashed curves show a fit assuming that all scaling violation comes from a term of the form aN/Q^2 with $a = .8 \text{ GeV}^2$. The QCD fit is excellent, but the fact that the dashed curve fits the data as well indicates that higher-twist effects could be significant.

Fig. 9. $xF_3(x, Q^2)$ at various Q^2 values. The CDHS data (Ref. [21]) were interpolated and placed into large bins for display purposes only. The solid curves are the QCD predictions based on integrating the Q^2 -evolution equation with the boundary condition $xF_3(x, 152.4 \text{ GeV}^2) = Cx^a(1-x)^b$. The dashed curves show a fit assuming that all scaling violation comes from a term of the form $\frac{d\sqrt{x}(1-x)^2}{Q^2}$ with $d = .4 \text{ GeV}^2$. As in Fig. 8, the QCD fits are excellent, but the fact that the dashed curves also fit the data indicates that higher-twist effects could be significant.

Fig. 10. Values of r_{NM} for various combinations of N and M from the data of Ref. [12]. Data points are shown for data with $Q^2 > 1 \text{ GeV}^2$ and for $Q^2 > 3 \text{ GeV}^2$. The lowest-order QCD predictions are indicated by solid horizontal lines while the shaded regions show a reasonable range for the second-order QCD predictions which are not precisely defined.

Fig. 11. The data (Ref. [12]) for $M_3(N, Q^2)$ are plotted versus the data for $M_3(M, Q^2)$ on a log scale. The solid curves are the predictions of leading-order QCD while the dashed curves (which are quite similar) are the results of using Eq. (4.11) with $a = 0.6$ and $b = 0.05$. This plot does not indicate the strong correlations between $M_3(N, Q^2)$ and $M_3(M, Q^2)$; the actual uncertainties are more like ellipses with their major axes along the curves.

Fig. 12. The values of $\alpha_s(Q^2)$ computed in second-order QCD using Eq. (4.14) with $\rho = 0$ (solid curve), $\rho = 2$ (dashed curve) and $\rho = -1.3$ (dash-dotted curve). This plot indicates that it is not meaningful to quote the value of $\alpha_s(Q^2)$ even within a given renormalization scheme without specifying the definition of Λ .

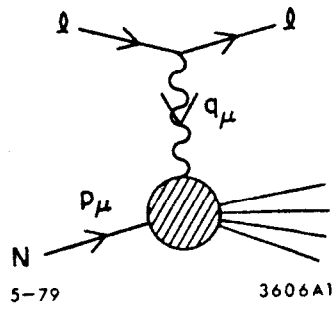


Fig. 1

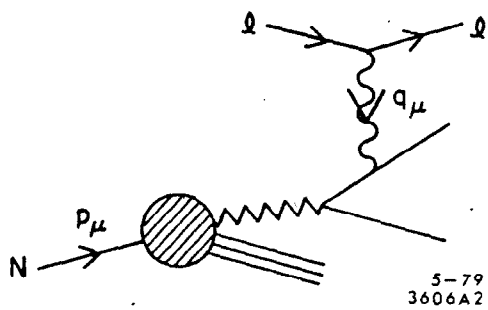


Fig. 2

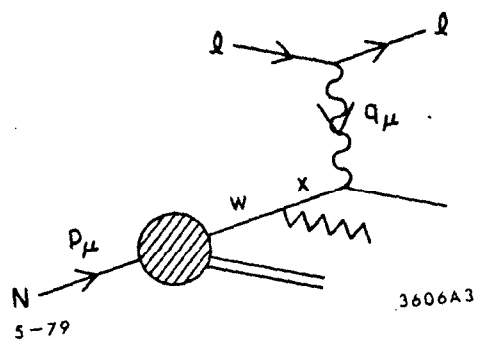
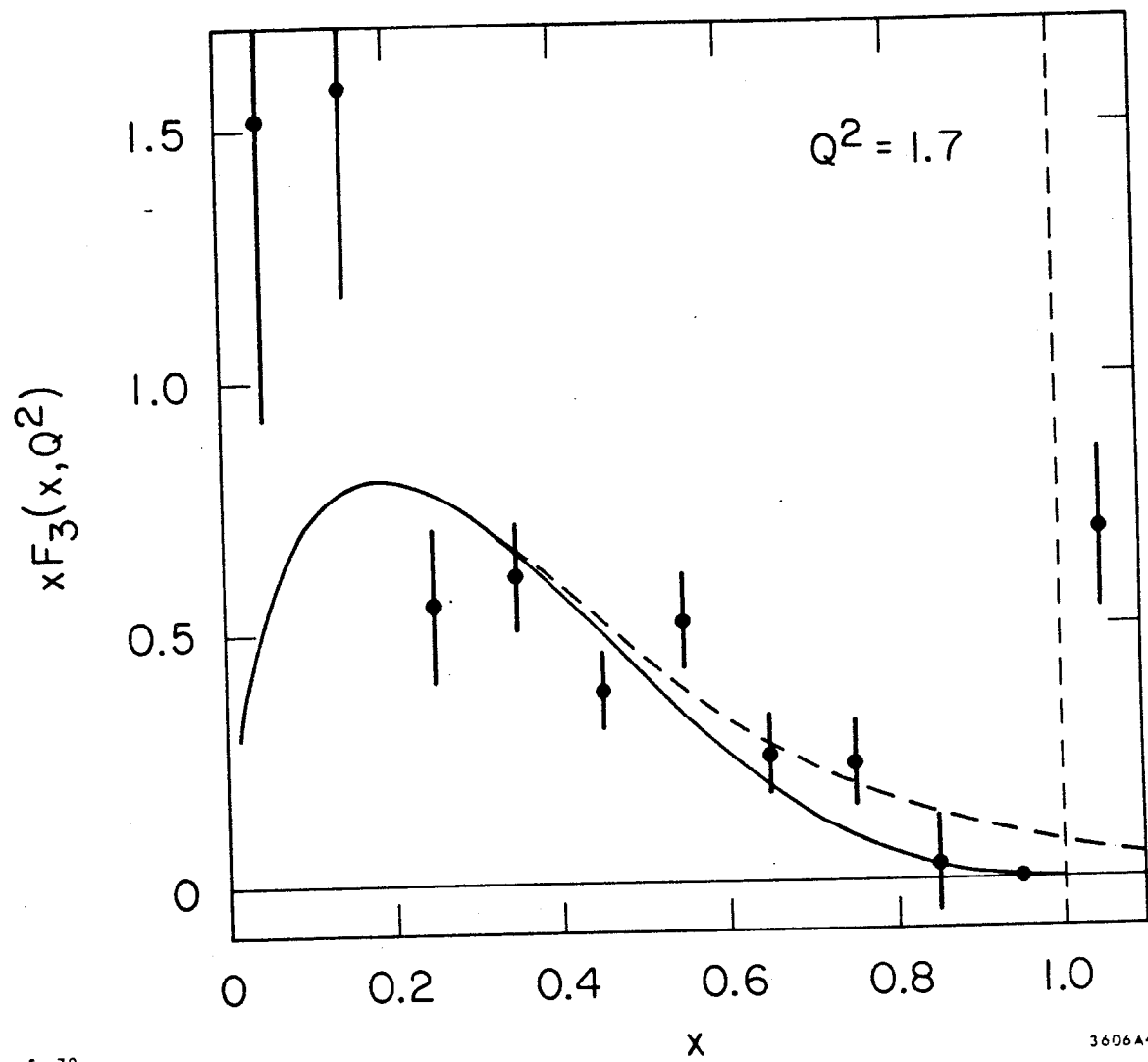


Fig. 3



5-79

3606A4

Fig. 4

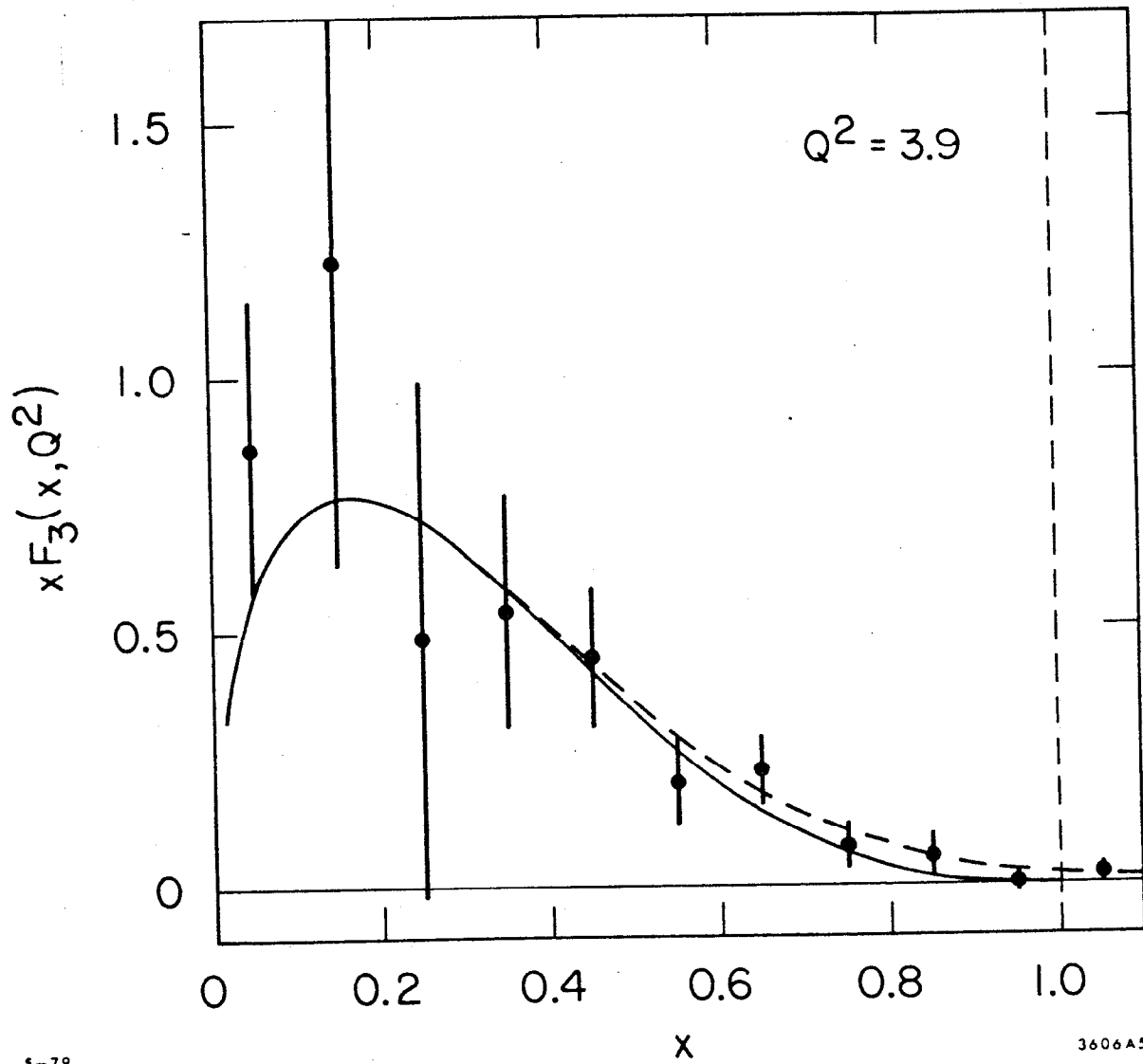


Fig. 5

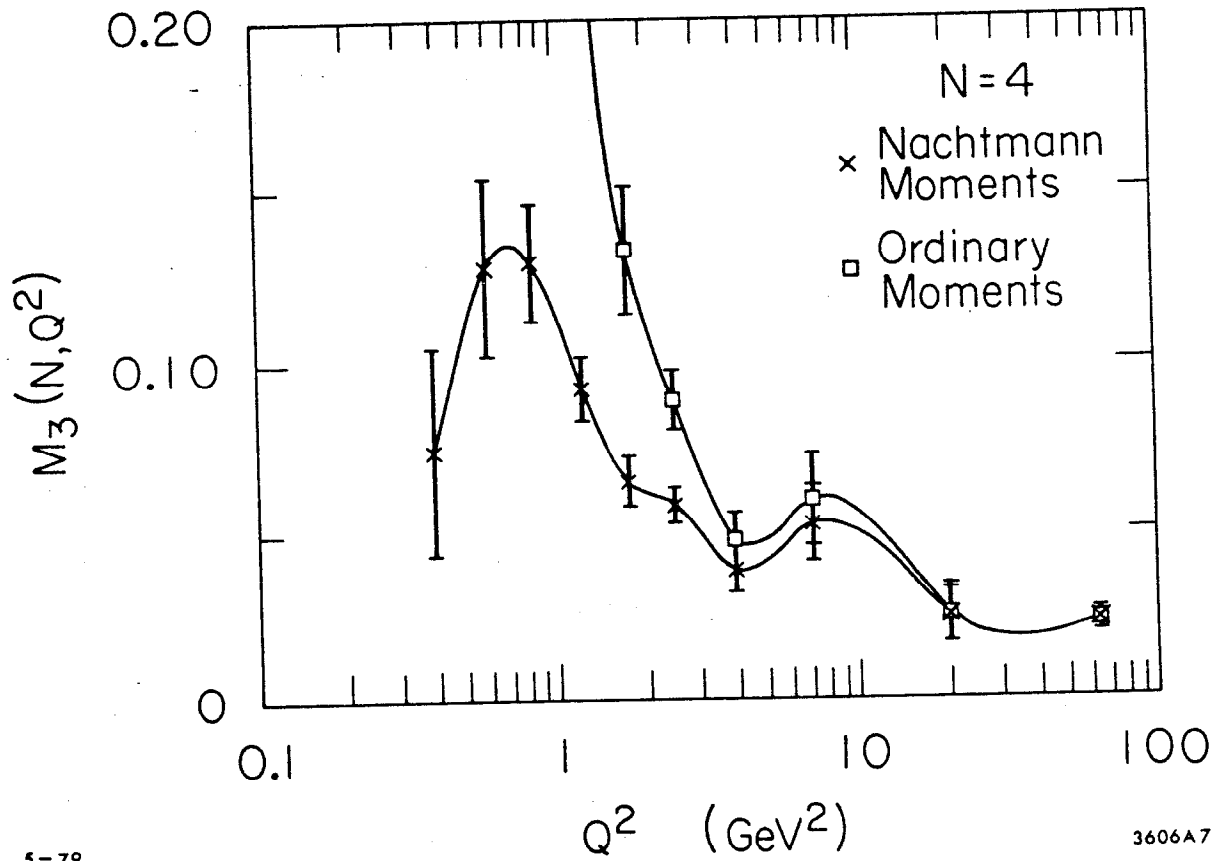


Fig. 6

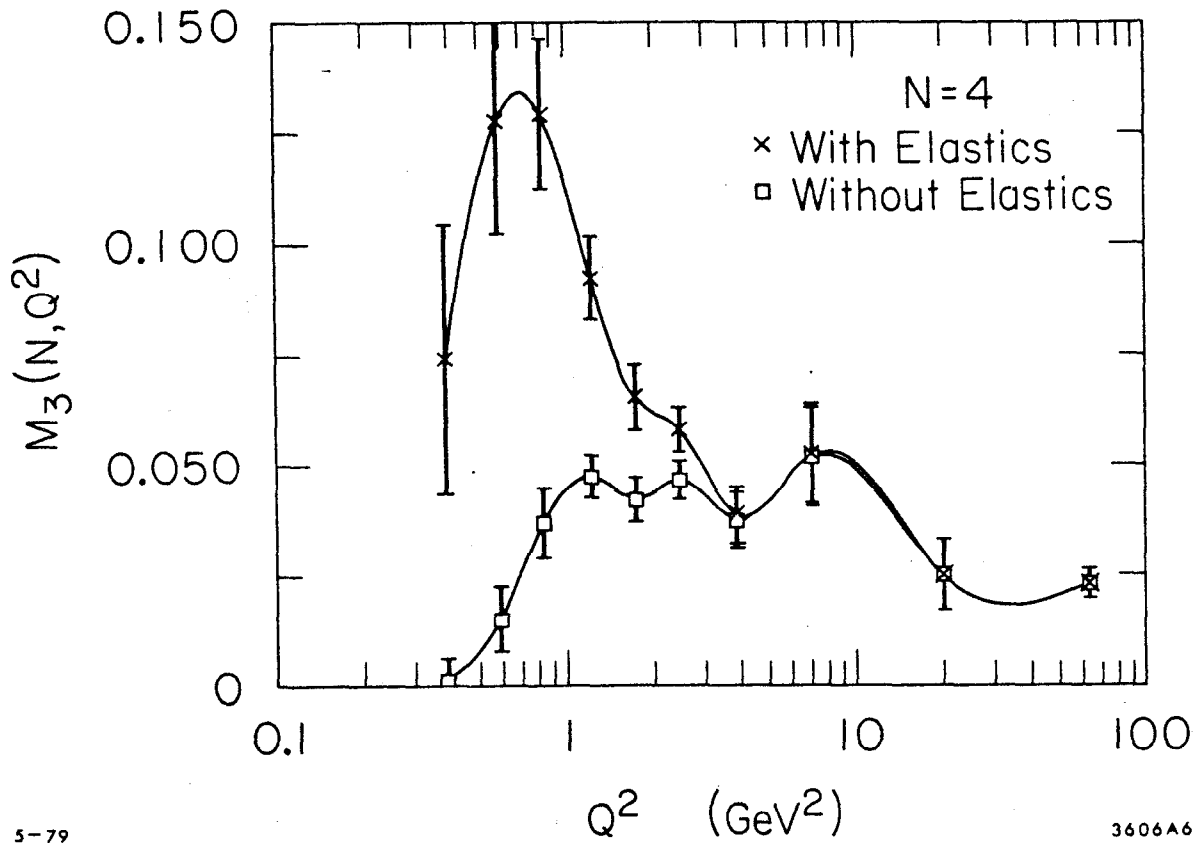


Fig. 7

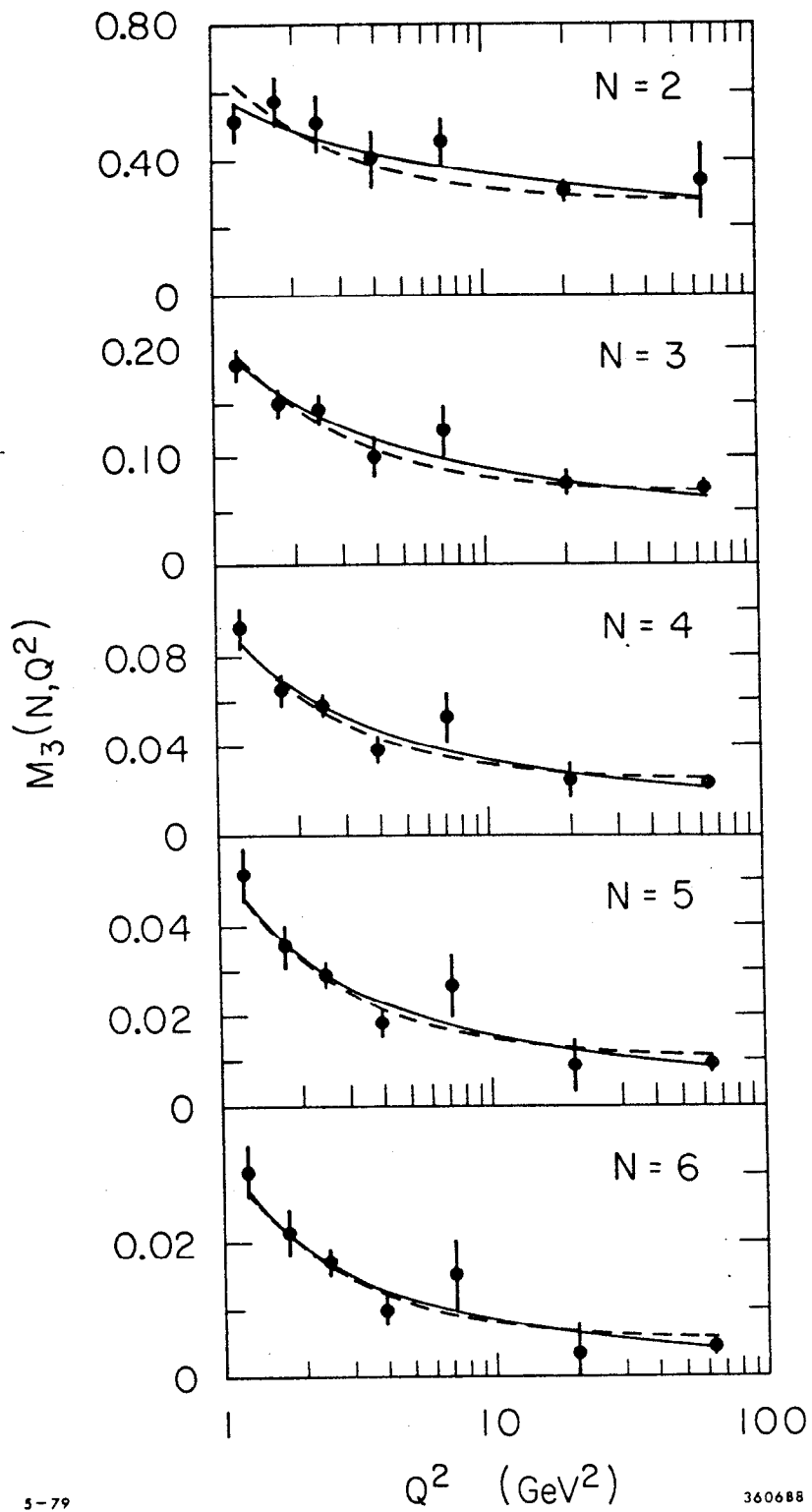
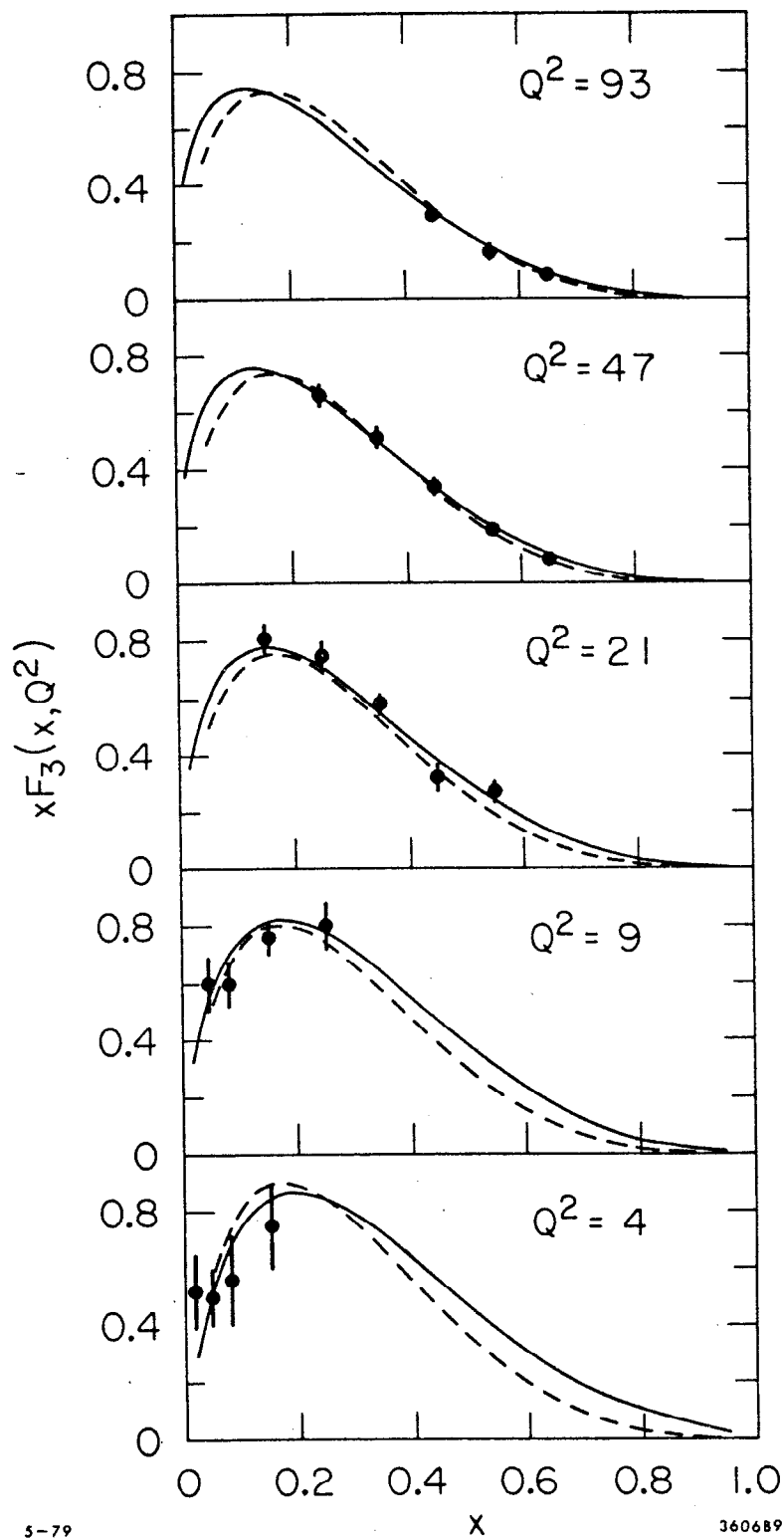


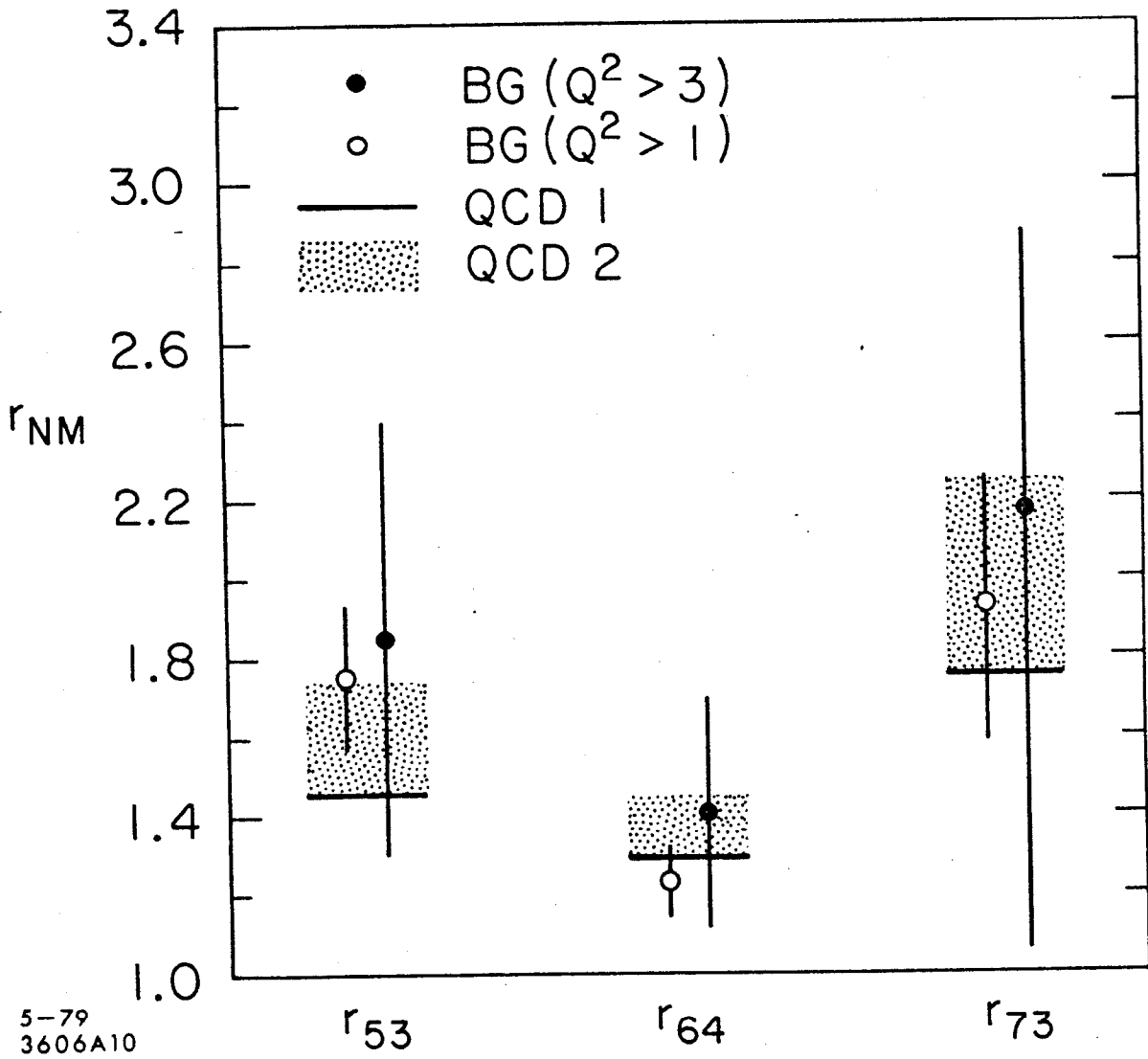
Fig. 8



5-79

360689

Fig. 9



5-79
3606A10

Fig. 10

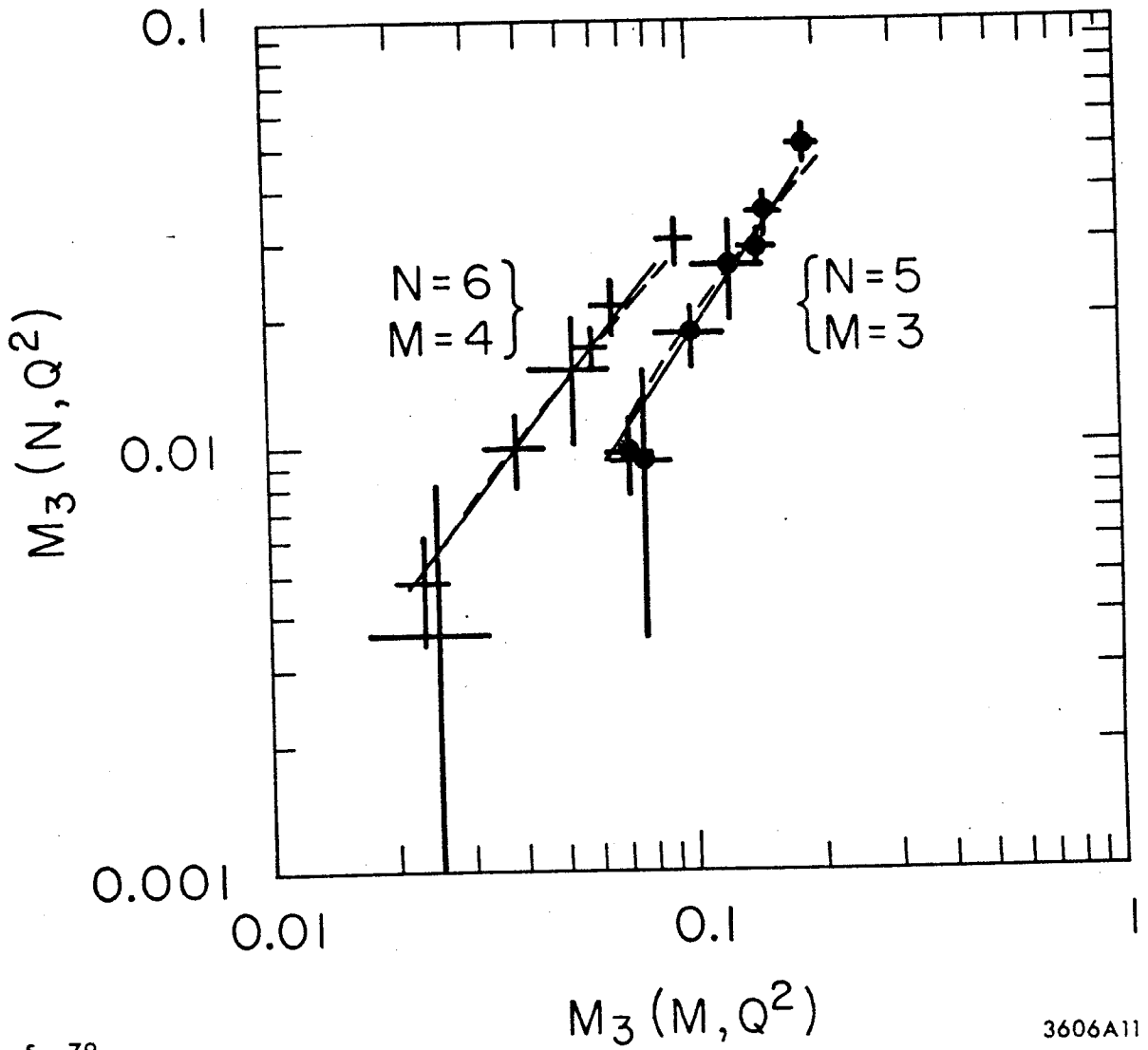
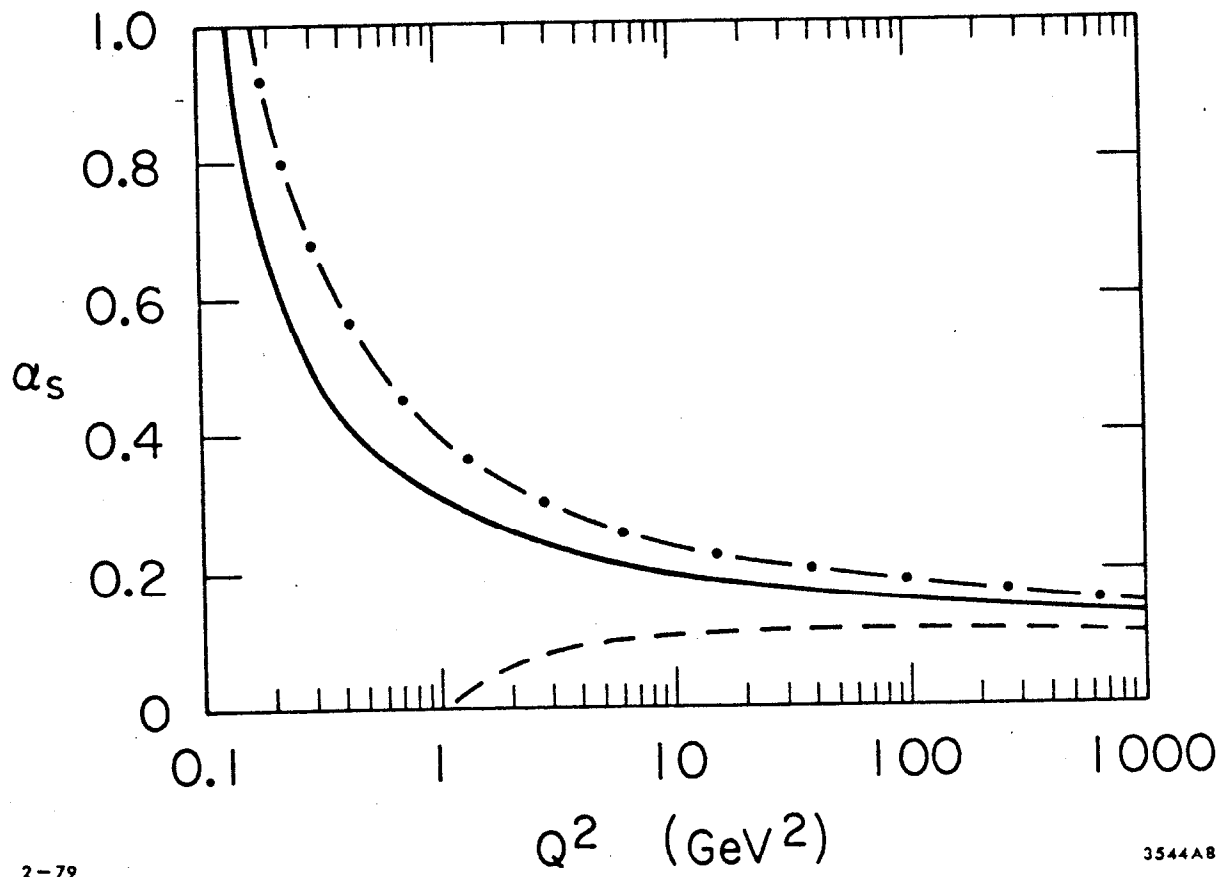


Fig. 11



2-79

3544A8

Fig. 12